FLORIDA STATE UNIVERSITY

COLLEGE OF ARTS AND SCIENCES

DILUTE SOLUTION PROPERTIES OF COPOLYMERS

By

IMAD A. HAIDAR AHMAD

A Thesis submitted to the
Department of Chemistry and Biochemistry
in partial fulfillment of the
requirements for the degree of
Master of Science

Degree Awarded:
Summer Semester, 2008

The members of the Committee approve the thesis of Imad Haidar Ahmad defended on March 20, 2008.

_____
André M. Striegel
Professor Directing Thesis

_____
Joseph B. Schlenoff
Committee Member

_____
Oliver Steinbock
Committee Member

Approved:

_____
Joseph B. Schlenoff, Chair, Department of Chemistry and Biochemistry

_____
Joseph Travis, Dean, College of Arts and Sciences

The Office of Graduate Studies has verified and approved the above named committee members.

ACKNOWLEDGMENTS

I would like to express my gratitude to my supervisor Dr. André M. Striegel. I am deeply indebted to him. Special thanks go to him for all the help, guidance, patience, encouragement, and motivation during these three years.

I would like to thank Dr. Schlenoff and Dr. Steinbock for being my committee members. I appreciate the time they spent for evaluating this thesis.

I would like to thank Seth Ostlund, an alumnus from our group, who helped me a when I first join Striegel's group. Also, I would like to thank the rest of Striegel's Group: Marcus Boon, Dustin Richard, Amanda Brewer, Michelle Smith, Shen Dong, and Samantha Isenberg.

I would like also to thank Professor Ali Safa who helped me applying to the graduate program at FSU.

I would like to thank two special persons in this world, my Dad (Amin Haidar Ahmad) and my Mom (Jamilie Haidar Ahmad). Besides, I would like to thank my brothers (Tarek and Rageb) and the loveliest sister in this world (Lozan). For all of them I dedicate this thesis.

Above all, Special thanks for my fiancée, Shereen Fakih. She is the person who stood beside me and encouraged me constantly. This accomplishment is as much hers as it is mine. Without her patience and sacrifice, this journey would have looked so much more intimidating.

TABLE OF CONTENTS

LIST OF TABLES

LIST OF FIGURES

LIST OF ABBREVIATIONS OR SYMBOLS

M ..... Molar mass

MMD ..... Molar mass distribution

[η] ..... intrinsic viscosity

A_2 ..... Second Virial Coefficient

R_G ..... radius of gyration

R_η ..... viscometric radius

R_H ..... hydrodynamic radius

R_T ..... thermodynamic radius

a ..... Mark-Houwink slope; indicates conformation

SLS ..... static light scattering

THF ..... Tetrahydrofuran

PS ..... Polystyrene

PMMA ..... Polymethyl methacrylate

SEC ..... Size Exclusion Chromatography

MALS ..... multi-angle light scattering

VISC ..... viscometric, viscometer

DLS ..... Dynamic Light Scattering

DRI ..... Differential Refractometer

dn/dc ..... refractive index increment

ABSTRACT

Copolymers comprise two different functionalities within one chain, arranged in different patterns according to the type of copolymer: Diblock, alternating, or random. The presence of these two different functionalities within the same chain enriches the copolymer properties and applications, and affects the copolymeric end-use properties. Copolymers are easily studied in dilute solution because otherwise interchain repulsion will be likely manifested.

In this study, size-exclusion chromatography (SEC) is coupled to multi-angle light scattering, viscometry, and refractometry detectors. From the wealth data produced from this triple-detector SEC system, we obtain information about the composition of the copolymers, their shape and size in solution, and their molar mass distribution.

In a controlled set of experiments, we characterize block, random, and alternating copolymers of polystyrene and poly(methyl methacrylate), as well as the constituent homopolymers. Different polymeric and copolymeric properties are studied using the triple detector system, such as: 1) The bulk percentage composition of copolymers is successfully calculated using an equation that relates the refractive index increments of the copolymer to that of the comprised homopolymers. This equation was derived for block copolymers, and we effectively extended its use to calculate the composition of the random and alternating copolymers as well. 2) Factors affecting the goodness of a solvent for copolymers are explained using their corresponding thermodynamic parameter. 3) The structure of the copolymers in solution is studied using relationships between either the radius of gyration and molar mass, or between intrinsic viscosity and molar mass. 4) Other polymeric properties, such as molar mass and molar mass distribution, are also determined.

CHAPTER ONE

INTRODUCTION

1.1-Copolymers: Definition and types

Copolymers are defined as macromolecules that compromise two different monomeric functionalities within one chain. The arrangement of the different functionalities within the polymeric chain corresponds to the different types of copolymers: Block when the two functionalities are assembled in the form of two blocks connected at one junction point, sequentially alternating in the alternating copolymer, and randomly distributed in the random copolymer. These different types of copolymers are shown in Figure 1.1, where the two different colors correspond to the different functionalities.

Block copolymer Random copolymer Alternating copolymer

Figure 1.1 The different types of copolymers

The three different types of copolymers possess different properties that affect not only their behavior in solution but also their end-use applications. These different applications are sometimes observed for different types of copolymers having the same chemistry but different monomeric arrangements. Some specific applications related to the different types of copolymers are: 1) block copolymers have potential in the area of drug delivery[1] due to the ability of a block copolymer to form micelles in solvents that are good for only one of the two monomers. 2) The capability of alternating copolymers to be used for delivering holes and electrons in light emitting diodes, due to their electrochemical stability which is related to the highly regulated arrangement of the monomers[2, 3] within the sequence. 3) The ability to reduce the surface tension between the fluids because of the efficiency of random copolymers to locate themselves at the interface of two immiscible phases.[4]

1.2-Why dilute solution?

A dilute solution is defined as a solution in which the solvated polymers are present in very low concentration, with the distance separating the polymeric chains from each other much larger than the size of the polymer in solution. With these two conditions fulfilled, interchain interaction between polymeric chains can be assumed to be negligible. Due to the ease of performing polymeric studies in dilute solution, these studies are used for deriving accurate properties of the polymers under more complicated conditions, as in the melt or in concentrated solutions, where the structure of a polymer is affected by interchain interactions. Characteristics of polymers derived from dilute condition studies are either relative properties dependent on the conditions of study or absolute properties related to the nature of the macromolecule. Examples of relative properties are the ability of different polymers to mix at the molecular level, which helps in understanding the polymerization process; the dimensionless radii ratios, which are absolute properties related to the conformation of the polymers in solution; behavior of the polymer under theta state pseudo-ideal conditions, where the linear polymer under these conditions is comparable to the conditions of the melt state.[5]

1.3- Dilute solutions of copolymers

Dilute solution studies of copolymers are more useful than nondilute solution studies, due to the fact that nondilute copolymeric solutions are complicated by the different types of intrachain and interchain interactions arising from the different functionalities incorporated within the same chain. Interactions in a copolymer are related to three different parameters: The molar mass, the relative percentages of each monomer, and the arrangement of monomers within a chain. Dilute solution properties of copolymers are important in determining the effect of the type of the copolymer (block, random, or alternating) and thus, the distribution of the monomers within the chain on the behavior and properties of the polymer. Under dilute solution conditions, the interchain interactions can be assumed to be negligible. In contrast, intrachain interactions can be

studied and quantified more accurately in the dilute regime than in the nondilute regime.[6-9]

Dilute solution studies are also used for testing the ability of copolymer to mix or phase separate from a matrix with a homopolymer. Studying the ability of different polymers to mix is important because: 1) Polymer blends are usually prepared in dilute solution then the solvent is evaporated, thus dilute solution changes to melt. 2) The polymerization process is performed in solution where the different monomers, the copolymer, and the initiator are in the same solvent; thus the ability to mix is critical for the copolymerization reaction to proceed[10-12].

Dilute solution studies are also used to find the percentage composition of each monomer in the polymeric chain. This is important due to the effect of the composition on the end use properties of the copolymer. The percentage composition affects physical properties such as size in solution, viscosity, refractive index, etc.

1.4- Copolymer applications.

Copolymers have wide range of applications due to: 1) The type of the copolymer (alternating, block, or random). 2) The ability to control chemical and physical properties by changing the percentage composition of the different monomers in the copolymer.

Intraocular lens implants. Copolymers containing reversible disulfide bonds have the ability to be liquefied when reduced or gelled when oxidized. The ability of these copolymers to switch between two different states under different conditions offers them the potential to be used in ophthalmologic applications, such as in intraocular lens implantation[13]. A natural ocular lens changes its physiological chemical content due to aging or stressing, thus resulting in irreversible changes in mechanical and optical properties of the lens. A good implant candidate should be a substance possessing by a properties comparable to these of natural eye, such as refractive index, transparency, elasticity, and biocompatibility[14]. Poly(acrylamide-*co*-*N*-*N*'bis(acryloyl)-cystamine), a

thiol-containing copolymer, forms a gel under physiological conditions and meets the prerequisites necessary for an implanted lens. The rate of gelling of these copolymers can be manipulated by controlling the percentage of SH groups, the concentration, and the molar mass of the polymer.[13]

Biomedical hydrogels. Hydrogels are water rich polymeric substances, usually used for biomedical purposes such as contact lens fabrication due to their clarity, flexibility, hydrophilicity, and high water content. Silicone hydrogels are used for contact lens fabrication due to the ability of oxygen to pass easily through the lens, thus nourishing the cornea and extending the maximum time contacts can be worn[15-18]. Copolymers are important for contact lenses fabrication because of the following: 1) Copolymers such as poly[2-hydroxyl methacrylate-*co*-methacrylic acid] are used as hydrogels. 2) Copolymers such as block copolymers of polyethylene oxide and polypropylene oxide are used as surfactants to increase surface wettability of the contact lens.[18].

Protein mimics. Random copolymers with hydrophilic and hydrophobic functionalities distributed throughout the chain are similar to proteins in the way that the polymer comprises groups with polarities similar to the hydrophilic carbonyl group and hydrophobic alkyl group in proteins. Protein-like copolymers were first predicted by computer simulation[19, 20], followed by actual synthesis. Poly[(*N*-vinylcaprolactam)-*co*-(*N*-vinylimidazole)], a catalyst used in studying the hydrolysis of ester substrates[21], was the first successful synthesized protein-like copolymer[22]. Protein-like copolymers are also used as models to study the localization, delocalization, or adsorption of proteins next to a lipid bilayer membrane. When adsorbed to a membrane surface, protein-like copolymers are used to study the relationships between the adsorption energy and the hydrophobicity of proteins.[23]

Viscosity index improve The viscosity of a copolymer solution is an adjustable property that depends on many parameters, such as molar mass and concentration, the thermodynamic state of solution, the percentage composition of the polymer, monomer chain length, and solvent additives [24, 25]. For example, the viscosity of acrylonitrile and

acrylamide copolymers dissolved in dimethyl sulfoxide changes with adding DMF and/or H_2O, or by adding KCl[24]. The potential of a copolymer to change its viscosity with changes in experimental conditions impart copolymers the ability to be used as viscosity index improvers. Butyl acrylate α-Olefin copolymers are oil viscosity index improvers, i.e. they provide for constant viscosity at different temperatures.[25]

Optical waveguides Candidates for waveguides should possess special physical, chemical, and mechanical properties, such as: adjustable refractive index, excellent transmission of light, thermal stability, and rigidity[26-28]. Copolymeric materials excel in optical waveguide fabrication because they can tune the different properties and because they can be stretched films. Examples of copolymeric optical waveguides are thin copolymeric films of octaflouropentyl methacrylate / hydroxyethyl methacrylate, styrene methyl methacrylate (S-MMA)[29] or of Styrene acrylonitrile[26, 27] have shown success in this field.

1.5- Why study Copolymers of PS-PMMA?

Monodisperse, as well as polydisperse standards of polystyrene (PS) and poly(methyl methacrylate) (PMMA) are commercially available. These polymers exist within wide molar mass ranges extending from the oligomeric region up to several million g/mol. As a result of the availability of these standards, the properties of these polymers such as their structure in solution, and intrinsic viscosity are well characterized for the individual molar masses along with the dependence of these properties on molar mass. This ability to characterize PS and PMMA facilitates the comparison of their individual properties as well as the properties of copolymers comprising these two functionalities.

There are several experimental reasons that support our choice of studying copolymers of PS and PMMA. The commercial availability of alternating, block, and random copolymers of PS and PMMA, added to the accessibility of selecting specific molar masses, percentage compositions, and polydispersities, enables the comparison of

copolymers based on the individual effects of molar mass and percentage composition on the second virial coefficient, A_2, values, and the effect of the percentage composition as well as the type of the copolymer on the refractive index increment, dn/dc, values.

This project will contribute to this growing field by integrating new ideas supported by experimental evidence including: 1) Using the dn/dc values to find the bulk percentage composition of the different types of the copolymers. 2) Showing differences in structure of the copolymer resulting from Mark-Houwink plots and conformation plots.

Copolymers of PS and PMMA functionalities have the power to self-assemble into regular patterns. These organized arrays include nanostructures such as lamellas and cylinders, which have found application as nanowires[30], as thin films with nanogrooves and nanopores[31-33], and in lithography[34]. As a result of the versatile applications of the copolymers comprising PS and PMMA, much research concerning the properties of these copolymers in the dilute and nondilute regimes is available[6, 9-12, 35-40].

1.6- Our approach

In this study alternating, block, and random copolymers of PS and PMMA are studied using two different types of experiments. The first type is done in offline mode, where the multi-angle light scattering detector (MALS) and the differential refractometer (DRI) are each used in batch mode to find bulk polymer solution properties. In the second type of experiment, an online size-exclusion separation module is coupled in series to the previous two detectors and to a differential viscometer (VISC), thus forming a triple-detector size-exclusion chromatography system. From the online experiments, characteristic distributions are determined for the bulk polymer quantities obtained from the offline mode. Other properties are also determined from the SEC/MALS/VISC/DRI online experiments as will be shown later.

The percentage composition of the copolymers was determined by relating the specific refractive index increments (dn/dc) of the copolymers to the dn/dc values of the

homopolymers. The dn/dc values of the polymers are determined from the DRI off-line experiment, and the equation used was originally derived for calculating the percentage composition for block copolymers. In this project, we successfully extended the application of this equation to quantitate the percentage composition of random and alternating copolymers.

Different factors affecting the goodness of copolymeric solutions, such as molar mass and percentage composition, are studied along with their effects. The second virial coefficient, A_2, is the thermodynamic parameter determined by the MALS off-line experiment and it is used to study the goodness of the solvent toward different homopolymers. Then, the thermodynamic parameters of the homopolymers are used to compare thermodynamic parameters among different copolymers. As a result of this comparison, factors affecting the thermodynamics of copolymeric solutions are determined as explained before.

From the on-line experiments, the triple detector contributes helps in determining important polymeric properties. Examples include: molar mass, molar mass distribution, intrinsic viscosity, and structure in solution. The structure of copolymers in solution is studied using two methods: 1) Relations between the radius of gyration and the molar mass. 2) The relationship between intrinsic viscosity and molar mass.

CHAPTER TWO

EXPERIMENTAL DESIGN

2.1 Instrument description

2.1.1- Size-exclusion chromatography

Chromatographic separation based on size began with J. Porath and P. Flodin in 1959 by proving the ability of a cross-linked gel to separate macromolecules according to their molecular size [41].

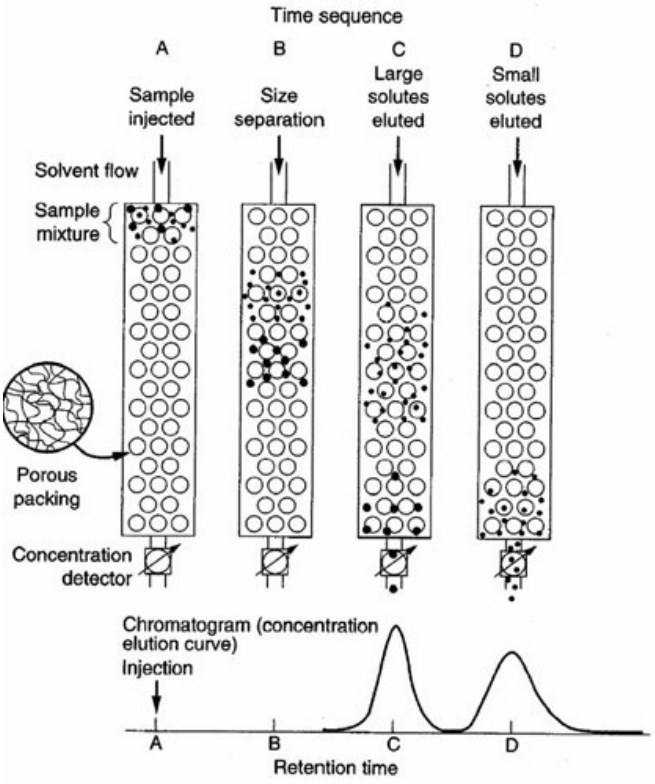

Figure 2.1 Size-exclusion chromatography (SEC)[42]

SEC is an-inverse sieving separation technique based on the fractionation of molecules according to their size in solution, where small molecules can access more pore volume inside the particles than larger molecules, resulting in the elution of the

larger molecules at an earlier time than the smaller molecules in a sample. The ability to separate different sizes is valid for a certain range of sizes, depending on the relative size difference between analyte and pore. This separation range is settled between a lower limit defined in the total exclusion limit and an upper limit of detection defined as the total permeation limit. The total exclusion limit can be determined from the signal of an analyte larger than the pore size of the packing material, while the total permeation peak is specified by the signal of a very small molecule compared to the pore size of the packing material. The size separation range of macromolecules in SEC can be related to the molar mass of the macromolecules by using standards of known molar mass, thus the SEC separation profile can be translated into a molar mass distribution via a retention time versus molar mass calibration curve.

The relation mentioned above relating the molar mass to molecular size is only valid for polymers of the same chemistry and structures as the standards. To solve the problem of finding standards of same chemistry and structure as the analytes, MALS is used as detection method for SEC because it is capable of determining the absolute molar mass. In this project, three detection methods are used online with SEC: Multi-angle light scattering (MALS), differential refractometry (DRI), and differential viscometry (VISC)[41-44].

2.1.2- Multi-angle light scattering (MALS) detector

Static light scattering (SLS) is a powerful analytical technique, capable of determining the absolute molar mass and size distribution of macromolecules as well as the thermodynamic state of the polymer solution. As shown in figure 2.2, the MALS photodiodes placed at different angles measure, at each angle, the excess Rayleigh ratio $R(\theta)$, defined as the amount of scattered light by the analyte in solution in excess of that scattered by the solvent. This scattering is related to the weight-average molar mass, M_w, of the analyte as per [43, 45, 46]

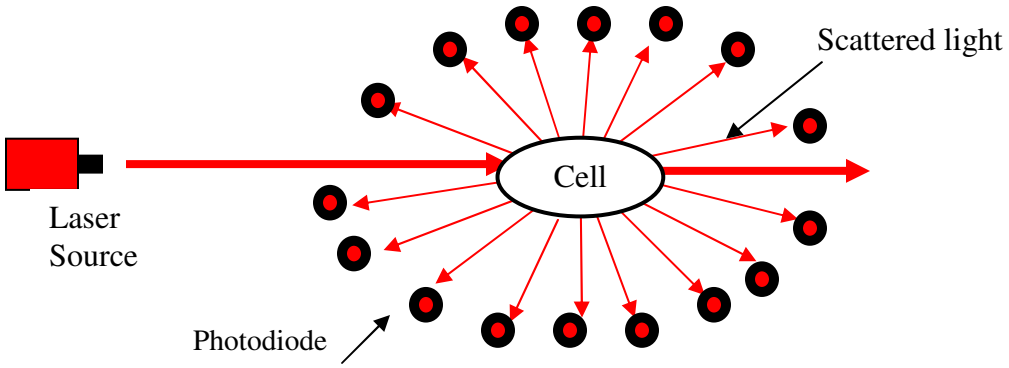

Figure 2.2 Multi-angle light scattering (MALS) - Top view

$$\frac{K^* c}{R_{(\theta)}} = \frac{1}{M_w P_{(\theta)}} + 2A_2 c + 3A_3 c^2 + \ldots \qquad (2.1)$$

$$\frac{1}{P_{(\theta)}} = 1 + \frac{16\pi^2}{3\lambda^2} \sin^2\left(\frac{\theta}{2}\right) \left\langle r^2 \right\rangle + \ldots \qquad (2.2)$$

$$K^* = \frac{4\pi^2 n_0^2 \left(\frac{dn}{dc}\right)^2}{N_A \lambda_0^4} \qquad (2.3)$$

where c is the concentration of polymer solution, $R_{(\theta)}$ is the excess Rayleigh scattering ratio, $P_{(\theta)}$ is the particle form factor, A_2 is the 2nd virial coefficient, K* is a constant defined in Eq (2-3), θ the scattering angle at which the observation is being made, $\langle r^2 \rangle$ is the mean-square radius of the polymer, n_0 is the refractive index of the neat solvent, dn/dc is the differential change in refractive index with the change in concentration, N_A is Avogadro's number, and $\lambda = \lambda_0/n_0$ is the wavelength of light in the medium, where λ_0 is the wavelength of light in vacuum.

There are two modes of operation in the MALS detector: The online mode works coupled to an SEC setup and the offline mode works independently. In the offline mode, the scattered light for different concentrations are measured at the sixteen different angles, and thus Rg, A_2, and M_w are obtained from Eq (2.1) and Eq (2.2). In the online

mode, MALS is capable of determining the molar mass distribution and the size distribution of a polymer when part of an SEC setup. One advantage of using a MALS photometer as an SEC detector, for the purposes of determining molar mass, is that M averages and distributions from SEC/MALS are absolute, i.e., calibration-independent. This contrasts with the calibrant-relative results obtained by SEC analysis using calibration curves[43, 45, 46].

2.1.3- Differential Viscometer (VISC)

The method of operation of the viscometer is based on the physical concept of Poiseuille's law, which relates the pressure drop of a solvent flowing through a tube of known length and radius to the viscosity of the solution through Eq.(2.4). Under the conditions that the solution is incompressible and the flow is laminar[41, 43, 47].

$$\Delta P = \frac{8 L \eta Q}{\pi r^4} \qquad (2.4)$$

where ΔP is the pressure drop across the tube, L is the length of the tube, η is the viscosity of the solution, Q is the volumetric flow of the solution, and r is the radius of the capillary.

The viscometer, as shown in fig 2.3, is designed with a wheatstone bridge design made up of four stainless steel capillary tubes (R_1, R_2, R_3 and R_4), two pressure transducers (ΔP and IP), a volume delay tube, and a heater exchanger to maintain constant temperature. The solution enters the Wheatstone bridge through the heat exchanger to stabilize the temperature (because viscosity is dependent on temperature), and then the solution splits into the two tubes R_1 and R_2. The solution flowing from R_1 toward R_4 is delayed inside the delay volume tube while the solution from R_2 continues uninterrupted toward R_3. The inlet pressure P_i is measured by the inlet pressure transducer IP. The drop in pressure is related to the presence of the analyte in the solution and is measured by the pressure transducer ΔP when the sample passes through R_3 and

the neat solvent passes through R_4. The measure of the drop in pressure drops is related to the specific viscosity η_{sp} (the increase in the viscosity of the solvent is due to the presence of the sample in solvent) according to equation [41, 43]

$$\eta_{sp} = \frac{4\Delta P}{P_i - 2\Delta P} \qquad (2.5)$$

Besides determination of η_{sp}, online viscometers are capable of determining other parameters such as the intrinsic viscosity, $[\eta]$, when coupled to a concentration-sensitive detector, and the viscometric radius, R_η, (the radius of a hard sphere that affects the solvent viscosity as much as the analyte does), when coupled to MALS. $[\eta]$ and R_η are defined according to the equations[5, 43]

$$[\eta] = \lim_{c \to 0} \frac{\eta_{sp}}{c} \qquad (2.6)$$

$$R_\eta = \left(\frac{3[\eta]M}{10\pi N_A} \right)^{1/3} \qquad (2.7)$$

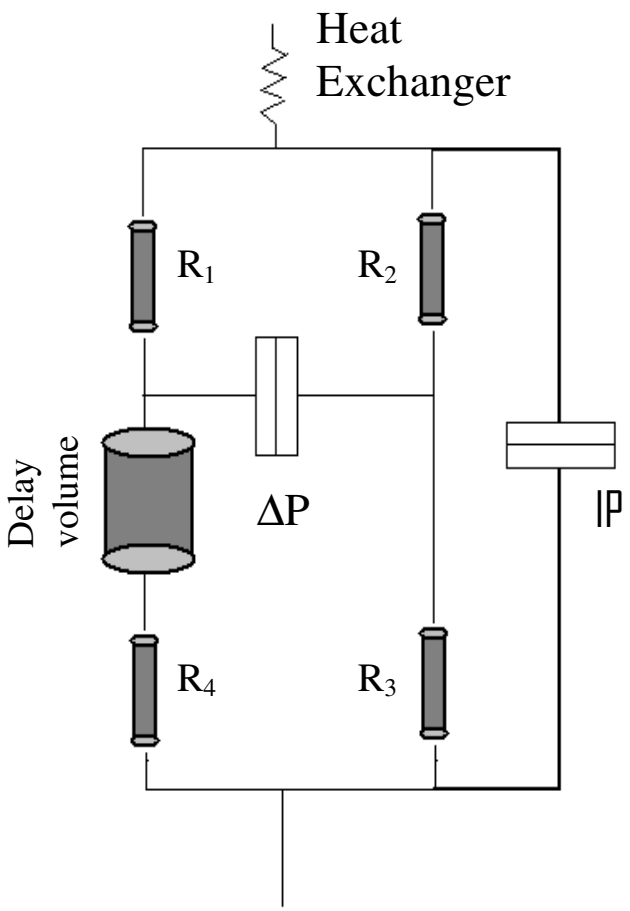

Figure 2.3 Wheatstone bridge viscometer design

2.1.4- Differential Refractometer (DRI)

The differential refractometer is the detector of choice for concentration measurements in SEC, due to the fact that it is a reliable, nondestructive detector, independent of flow rate, and universal. The physical basis of detection in refractometry is dependent on the relation between the concentration of the analyte in solution and the angle of refraction of the light passing through the solution. The change in concentration results in a change of the refractive index of the solution from that of the solvent and thus results in a shift in the angle of refraction of light from the angle of incidence as indicated by equation 2.8 [48].

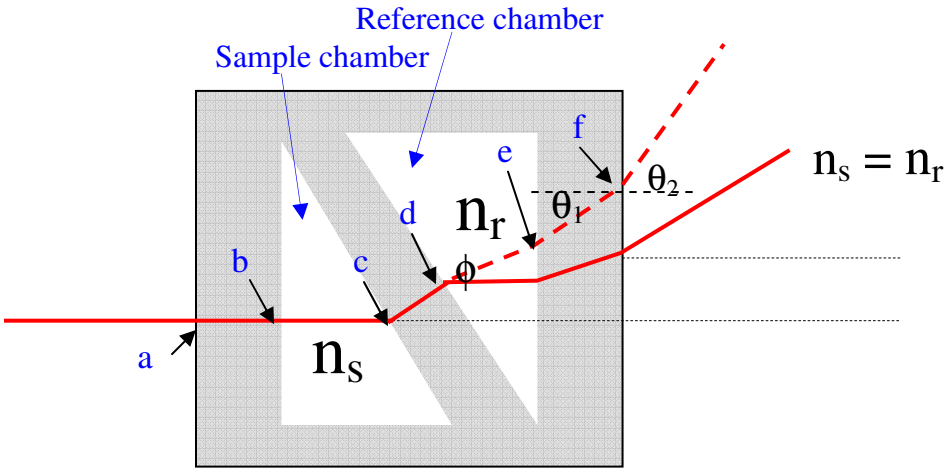

Figure 2.4 Differential Refractometer.

In a refractometer there are two compartments, one for the sample to flow through and the other for the reference solvent (figure 2.4). According to Snell's law expressed in equation (2.8), the light directed from one medium to another will be refracted at the interface between the different mediums depending on the difference between the refractive indices of these two mediums. Consequently, the light will be diffracted at six different positions as labeled from (a) till (f) in figure 2.4. At each of these interfaces, Snell's law can be applied relating the angle of incidence to the angle of refraction where each of these angles is defined as the angle between the light beam and the normal line at the interface. An example is shown at the point (f).

The process of measuring the concentration of the analyte in the reference is done in two steps. First, both reference and sample compartment are filled with the neat solvent, and the position of the diffracted beam is denoted as position zero as indicated by angle ϕ in the figure. Second, the sample cell is filled with the sample solution while the neat solvent is still trapped inside the reference sample. As the sample solution travels through the sample cell, the angle of diffraction shifts from the zero position giving a new angle of diffraction (α). The overall angle deviation is related to the concentration of the analyte in the solution according to equation 2.9, where n is the refractive index of the

solution, n_o is the refractive index of the pure solvent, and n_a is the refractive index of the analyte.

$$n_1 \sin\theta_1 = n_2 \sin\theta_2 \qquad (2.8)$$

$$C = \frac{n - n_0}{n_a - n_0} \qquad (2.9)$$

The increased sensitivity of modern refractometer is due to the use of photodiode arrays to determine the angle of diffraction. This enhances the sensitivity of the refractometer by more than a factor of 200 relative to the old refractometers which used two photodiodes. Additionally, DRI is capable of measuring the dn/dc, defined as the differential change in the refractive index of the solution as the concentration of the analyte in solution changes. Dn/dc values can be determined either offline, by injecting samples with different concentrations, or online by assuming a 100% mass recovery. The dn/dc values are necessary for the determination of absolute Mw using static light scattering techniques, as per equations (2.1)-2.3).

2.2- Description of experiments:

2.2.1-Off-line experiments

In off-line mode, the detector is decoupled from the separation setup, and a series of dissolutions are injected directly into the detector. As a result of the absence of a separation technique, only average (bulk) properties of the entire polymer (or polymer solution) are obtained from this mode of analysis. Two types of off-line experiments were performed: The dn/dc experiment using the differential refractometer (DRI), and the Zimm plot experiment using the multi-angle light scattering (MALS) detector.

Dn/dc experiments are important for determining the refractive index increment (dn/dc) of polymer. We use this datum to calculate the percentage composition of the copolymer, by relating the (dn/dc)s of the copolymers and the (dn/dc)s of their

constituent homopolymers. Besides using dn/dc to calculate the percentage composition of a copolymer, dn/dc values are essential for calculating concentration and molar mass of a polymer, as will be explained in Section 4.1.

Zimm plots are important for determining the second virial coefficient (A_2) which evaluates the ability of a solvent to dissolve and solvate a polymer. Factors affecting the A_2 values of copolymers, such as molar mass and composition, are studied by comparing the A_2 of the copolymers to those of their corresponding homopolymers. In addition to the A_2 values obtained from the Zimm plot, average values of molar mass and radius of gyration are also determined.

2.2.2-On-line experiments (SEC/MALS/VISC/DRI)

In online mode, the separation technique enables fractionating the sample according to molecular size. An advantage of online over off-line experiments is the ability to obtain the distribution of properties, instead of property average obtained by the offline experiments. Examples of properties acquired from the online SEC/MALS/VISC/DRI are: 1) Distribution of molar mass. 2) Distribution of intrinsic viscosities. 3) Distribution of the radius of gyration. These distributions are important to obtain plots such as the Mark-Houwink plots of the intrinsic viscosity versus molar mass and the conformation plots of the radius of gyration versus the molar mass. From these plots, we can determine the structure of a polymer or copolymer in solution.

CHAPTER THREE

EXPERIMENTAL

3.1- Materials

For this study, we chose two polystyrenes (PS), two poly(methylmethacrylates) (PMMA), and the following copolymers of PS and PMMA: Two block copolymers (PS-*b*-PMMA), two random copolymers (PS-*co*-PMMA), and two alternating copolymers (PS-*alt*-PMMA). The structures of the styrene and methyl methacrylate monomers are shown in figure 3.1. The molar mass, polydispersity, and percentage composition of the polymers we chose for this study are shown in table 3.1.

Table 3.1- Polymers used in this study

Polymer used	M_w/M_n	% of PS	Source
PS (49K)	1.01	100	Polymer Laboratories
PS (133K)	1.01	100	Polymer Laboratories
PMMA (53K)	1.01	0	Polymer Laboratories
PMMA (138K)	1.03	0	Polymer Laboratories
PS-*b*-PMMA (46K, 138K)	1.06	25[a]	Polymer Source
PS-*b*-PMMA (131K, 46K)	1.02	75[a]	Polymer Source
PS-*co*-PMMA (Mn 126K)	1.39	20[b]	Polymer Source
PS-*co*-PMMA (Mn 186K)	1.43	25[b]	Polymer Source
PS-*alt*-PMMA (Mn 235K)	1.85	50[b]	Polymer Source
PS-*alt*-PMMA (Mn 561K)	1.94	50[b]	Polymer Source

[a] Percentages are calculated using the molar mass of each block

[b] Values from the manufacturer

For the homo and random copolymers, the numbers in parenthesis correspond to peak average molar mass (homopolymers) and to the number-average molar mass (random copolymers), whereas for the block copolymers the first and second values

within the parenthesis correspond to the molar masses of the PS block and the PMMA block, respectively. The M_w/M_n values are the polydispersities of these polymers. M_w/M_n generally correspond to the breadth of the molar mass distribution, the larger the polydispersity, the broader the molar masses are distributed. PS, PMMA, and the block copolymers all have narrow polydispersities, while the random and alternating copolymers have relatively broad polydispersities.

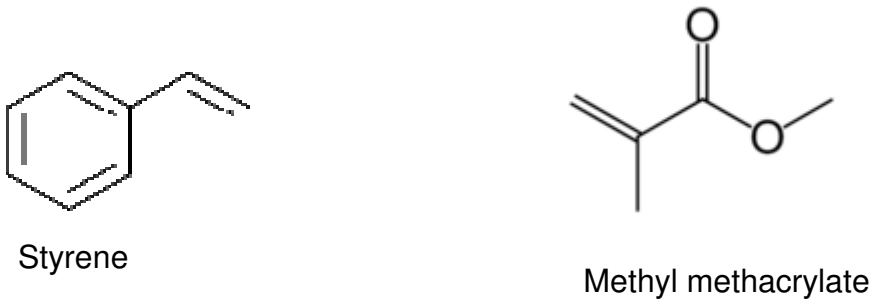

Figure 3.1- Styrene and Methyl methacrylate monomers

Tetrahydrofuran (THF) inhibited with BHT was used as solvent and mobile phase and was purchased from EMD Chemicals Inc. Methanol, purchased from VWR international, was used to flush and lubricate the tubes and ports in the Waters 2695 separation module. PTFE syringe filters for the offline experiments (0.02 μm for solvent and 0.45 μm for polymer solutions) were purchased from VWR international.

3.2- Online Experiments (SEC/MALS/VISC/DRI)

For the online experiments, a concentration of 1 mg/mL was prepared and left on a laboratory wrist-action shaker over night. For increased precision, two different 1 mg/mL solutions of each polymer were prepared and, from each dissolution, two injections were performed, for a total of four injections for each polymer. The SEC module consisted of a Waters 2695, three SEC columns (PLgel 10 μm mixed bead, Polymer laboratories), and three detectors in series starting with the MALS detector followed by a VISC and the DRI is the last detector in this setup. (All these detectors are from Wyatt, Santa Barbara, California.). The software used for acquiring and analyzing the data was ASTRA 5.3.2.12 from Wyatt technology Corporation (WTC).

3.3- Off-line determination of dn/dc:

For the offline dn/dc determinations, at least 5 different concentration for each sample, ranging from 0.2 to 7 mg/mL, are injected into the differential refractometer using Razel model A-99EJ syringe pump, starting with the neat solvent filtered through 0.02 µm syringe filters and followed by the series of the concentrations starting from the lowest to the highest, with all polymeric solutions filtered through 0.45 µm syringe filters. The polymers are dissolved in THF and left overnight on the wrist-action shaker to make sure that all the polymers are fully solvated. The data collection and processing is performed using Astra software.

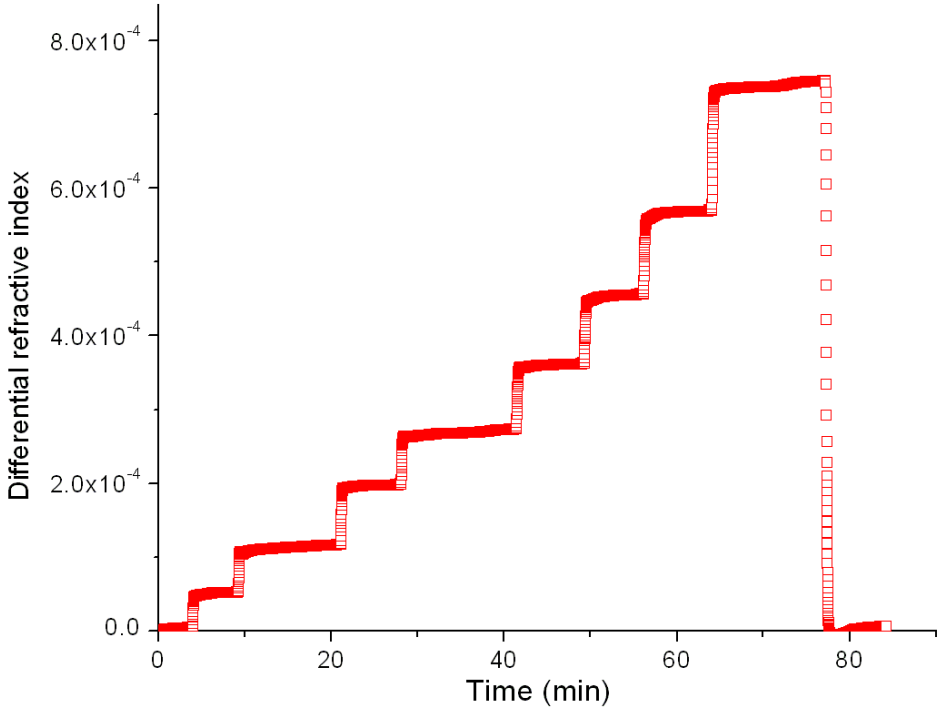

Figure 3.2-DRI vs time for PS 186K

To better understand the dn/dc experiment, figure 3.2 shows the DRI response as a function of time for a particular homopolymer of styrene, PS 186K. The first and last plateaus correspond to the neat solvent and they are used for baseline determination. The eight plateaus enclosed between the solvent plateaus correspond to the different dissolutions used in this offline experiment. The increase in the detector response going from one plateau to the next corresponds to the increase in the sample concentration. From this figure, the detector response related to each concentration can be obtained by subtracting the response related to the neat solvent (i.e. by subtracting the solvent plateau from each of the individual injection plateaus), and then this normalized response is plotted against the concentration of each sample, as shown in figure 3.3. From this new graph, dn/dc can be obtained as the slope of the plot of differential RI versus concentration. The dn/dc which is a value needed to accurately quantitate the data from our SLS experiments, as described in chapter two.

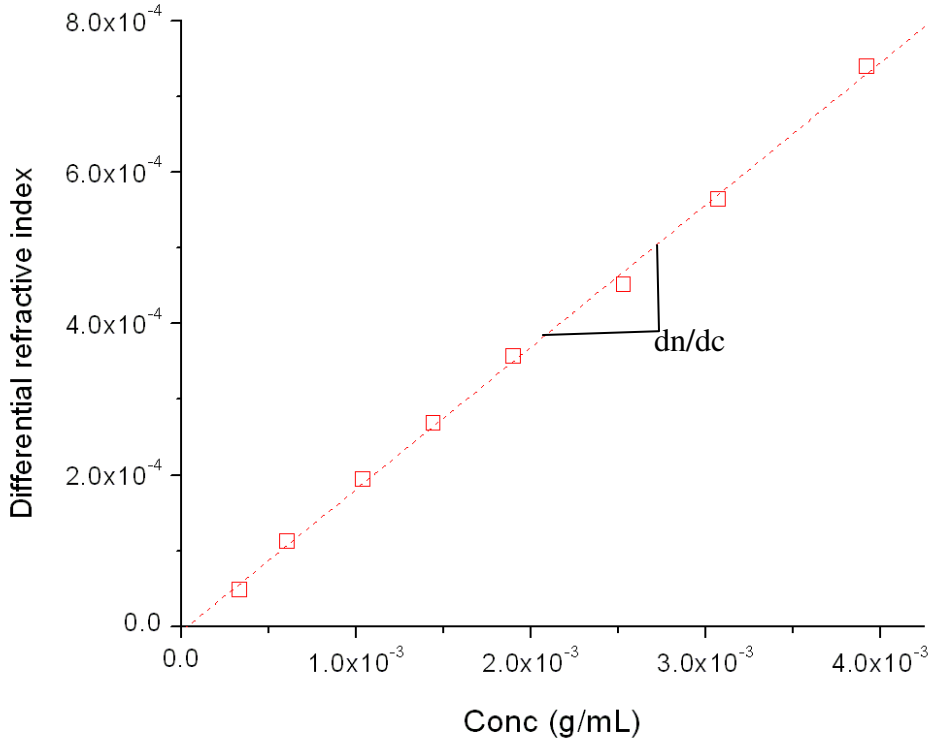

Figure 3.3-DRI vs Concentration for PS186K

3.4- Offline MALS determination

The main purpose for doing the off-line MALS experiment is the determination of the second virial coefficient (A_2) of the polymers at the experimental solvent/temperature conditions. Using the Razel model syringe pump, the samples prepared for the dn/dc experiments were injected directly into the MALS photometer, starting with the lowest concentration and proceeding toward the highest one. For baseline settings, the neat solvent was injected before and after the samples as was the case for the dn/dc determinations described in the previous section. The solvent was filtered through 0.02 μm filters, while the samples were filtered through 0.2 μm filters. Flow rate was 0.1 mL min^{-1}. A narrow polydispersity 31K PS sample (M_w/M_n=1.03) is used to correct the difference between the detector output scattering voltages. The 31K PS sample was used because it is an isotropic sample that scatters light in equal efficiency in all directions. The Astra software used for acquiring the data is also used for obtaining a Zimm plot, shown in figure 3.5.

Figure 3.4 is a good visual aid to understand the off-line MALS experiment. This figure shows the response of the 90° photodiode as a function of time. The first and the last plateaus on this plot correspond to the neat solvent injected before and after the samples. The ladder-like plateaus correspond to the different dissolutions used in this experiment and the plateau at 80 minutes corresponds to the sample used for normalizing the photodiodes. The increase in the detector response corresponds to the increase in the concentration. Using the equations in section 2.1.2, the Zimm plot shown in figure 3.5 can be derived from the data shown in figure 3.4. In this Zimm plot, the horizontal lines connect the different concentrations used in this determination, while the vertical lines connect the data obtained from the different photodiodes (i.e, connect the angular data). A stretching factor, kc, is inserted to the x-axis data to improve the visual clarity of the plot. The red-colored horizontal line corresponds to the extrapolation of the data to a concentration equal to zero, while the green vertical line corresponds to the extrapolation

of the angular data to zero angle. The slope of green line is proportional to the second virial coefficient, while the slope of the red line is proportional to the radius of gyration. The intercept of the two lines is proportional to $Mw^{-1.}$

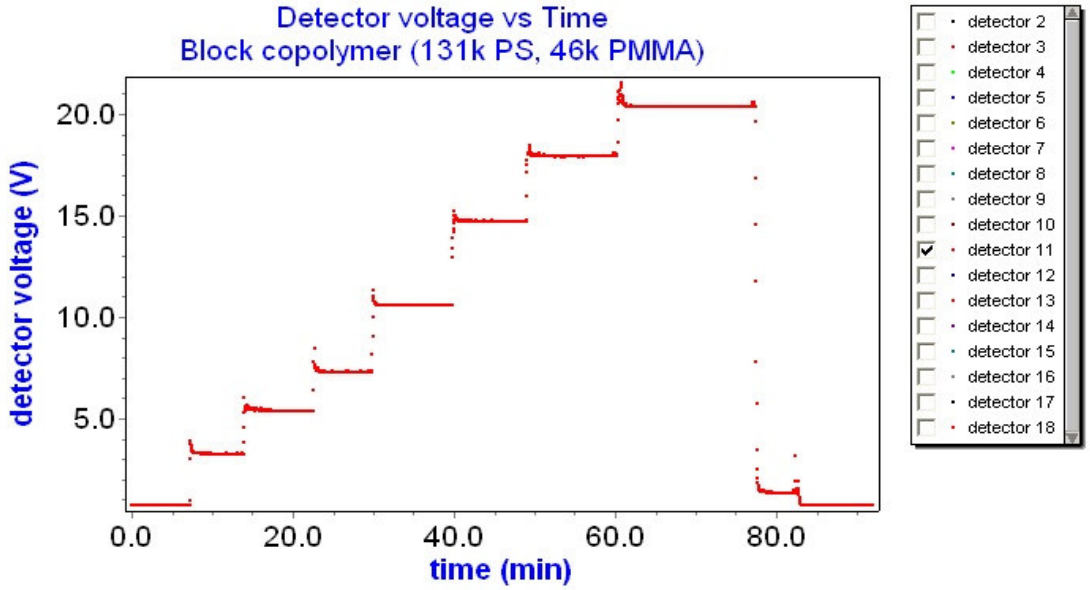

Figure 3.4- Detector voltage for 90° photodiode vs time

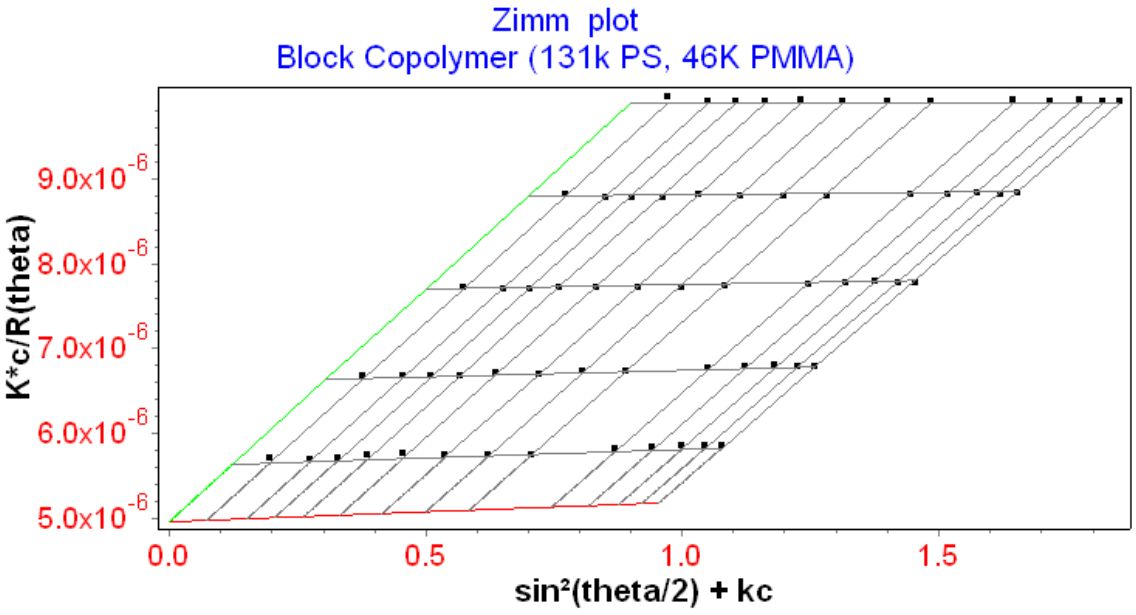

Figure 3.5- Zimm plot

CHAPTER FOUR

POLYMERIC AND COPOLYMERIC DILUTE SOLUTION PROPERTIES

4.1 – Specific refractive index increment (dn/dc) results:

The specific refractive index increment is defined as the change in the refractive index of a solution resulting from the change in polymer concentration. The dn/dc is an essential parameter to determine many physical and chemical properties such as: 1) Calculation of the concentration of the polymer using the refractive index of the solution, or vice-versa. 2) Determining the absolute molar mass of the polymer. 3) Characterizing the size and shape of the polymer.

Table 4.1- dn/dc values for the polymers

Polymer	**dn/dc (mL/g)**
PS (49K)	0.190 ± 0.002
PS (133K)	0.192 ± 0.002
PMMA (53K)	0.084 ± 0.001
PMMA (138K)	0.090 ± 0.001
PS-*b*-PMMA (46K, 138K)	0.109 ± 0.001
PS-*b*-PMMA (131K, 46K)	0.168 ± 0.001
PS-*co*-PMMA (Mn 126K)	0.108 ± 0.004
PS-*co*-PMMA (Mn 186K)	0.111 ± 0.002
PS-*alt*-PMMA (Mn 235K)	0.136 ± 0.002
PS-*alt*-PMMA (Mn 561K)	0.137 ± 0.001

Table 4.1- dn/dc values for the polymers

In this section, we will quantify the percentage composition of the copolymers by relating their dn/dc values to those of their corresponding homopolymers. The dn/dc values of the copolymer and the homopolymers are determined by using a differential refractometer off-line, as described in section 3.3. These values shown in table 4.1.

4.1.1 - dn/dc as a function of molar mass for homopolymers:

For each homopolymer, polystyrene or poly(methyl methacrylate), dn/dc values appear to be independent of molar mass. This is due to the negligible effect of end groups on the overall electronic environment of the polymer outside of the oligomeric region. [49, 50]

4.1.2 - dn/dc values of block copolymers

For the block copolymers, the percentage of PS and PMMA blocks and the dn/dc of the individual homopolymers can be used to calculate the dn/dc of the block copolymers as per [51]

$$(dn/dc) = (dn/dc)_a w_a + (dn/dc)_b w_b \qquad (4.1)$$
$$(dn/dc) = (dn/dc)_a w_a + (dn/dc)_b (1 - w_a) \qquad (4.2)$$

Where a and b correspond to the two functionalities in a copolymer, w_a is the percentage of monomer a in the copolymer, and w_b the percentage of monomer b in the copolymer[51]. Results of these calculations are shown in table 4.2 below.

Table 4.2- calculated and measured dn/dc values of the block copolymers

Polymer	**DP of PS**	**DP of PMMA**	**% of PS**	**% of PMMA**	**Calculated dn/dc (mL/g)**	**measured dn/dc (mL/g)**
PS-*b*-PMMA (46K, 138K)	442	1378	24.3	75.7	0.112	0.109 ± 0.002
PS-*b*-PMMA (131K, 46K)	1258	459	73.3	26.7	0.163	0.168 ± 0.001

If the dn/dc values of block copolymers been are already available, the above equation can also be used also to back-calculate the percentage composition of the block copolymers. Results of this are shown in table 4.3. The percentage of PS was calculated based on equations 4.1 and 4.2 and values of dn/dc for the block copolymers obtained from off-line DRI experiments, as described in section 3.3.

Table 4.3- back calculating the % composition of the block copolymers.

Polymer	**dn/dc (mL/g)**	**Finding the % of PS (X)**	**Calculated mole % of PS**	**% of PS***
PS-*b*-PMMA (46K, 138K)	0.109 ± 0.002	0.109= 0.191X+0.087(1-X)	21.2 ± 2.2	24.3
PS-*b*-PMMA (131K, 46K)	0.168 ± 0.001	0.168= 0.191X+0.087(1-X)	77.9 ± 2.2	73.3
* Percentages determined using molar mass of PS and PMMA blocks.				

From the above calculations we can conclude that the dn/dc is an additive property of block copolymers as a function of the percentage composition of each block. The dn/dc plots of block copolymers and homopolymers (figure 4.1) show how the dn/dc trends of block copolymers fit within those of the homopolymers. The location of the dn/dc plots of a block copolymer with respect to the homopolymers is indicative of the percentage composition of the copolymer. As can be seen in figure 4.1, the dn/dc plots of block copolymers rich in PS are closer to dn/dc plot of PS homopolymer than that to the plot of PMMA homopolymer.

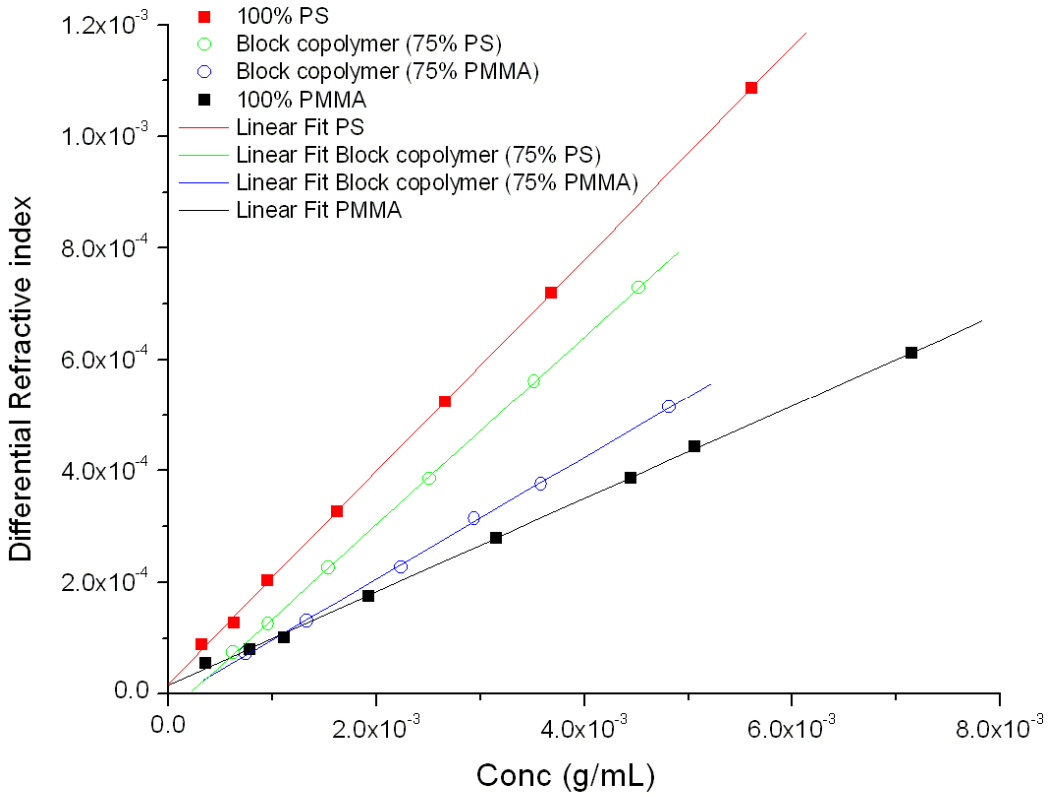

Figure 4.1- dn/dc plots of the block copolymers and their corresponding homopolymers.

4.1.3 - dn/dc of random copolymers

The dn/dc overlay plot of the random copolymers and the homopolymers in figure 4.2 indicates that the random copolymers are richer in PMMA than in PS, as indicated by the dn/dc plots of random copolymers being nearer to the dn/dc plots of pure PMMA than to the plots of pure PS. The method used for back-calculating the percentage composition of the block copolymer eq. 4.2 can be also used here.

Table 4.4- back calculating the % composition of the random copolymers.

Polymer	dn/dc (mL/g)	Finding the % of PS (X)	Calculated mole % of PS	Mole % of PS*
PS-*co*-PMMA (Mn 126K)	0.108 ± 0.004	0.108= 0.191X+0.087(1-X)	20.2 ± 4.0	20%
PS-*co*-PMMA (Mn 186K)	0.111 ± 0.002	0.111= 0.191X+0.087(1-X)	23.1 ± 2.2	25%
* Percentages determined by the manufacturer using ^{1}H-NMR.				

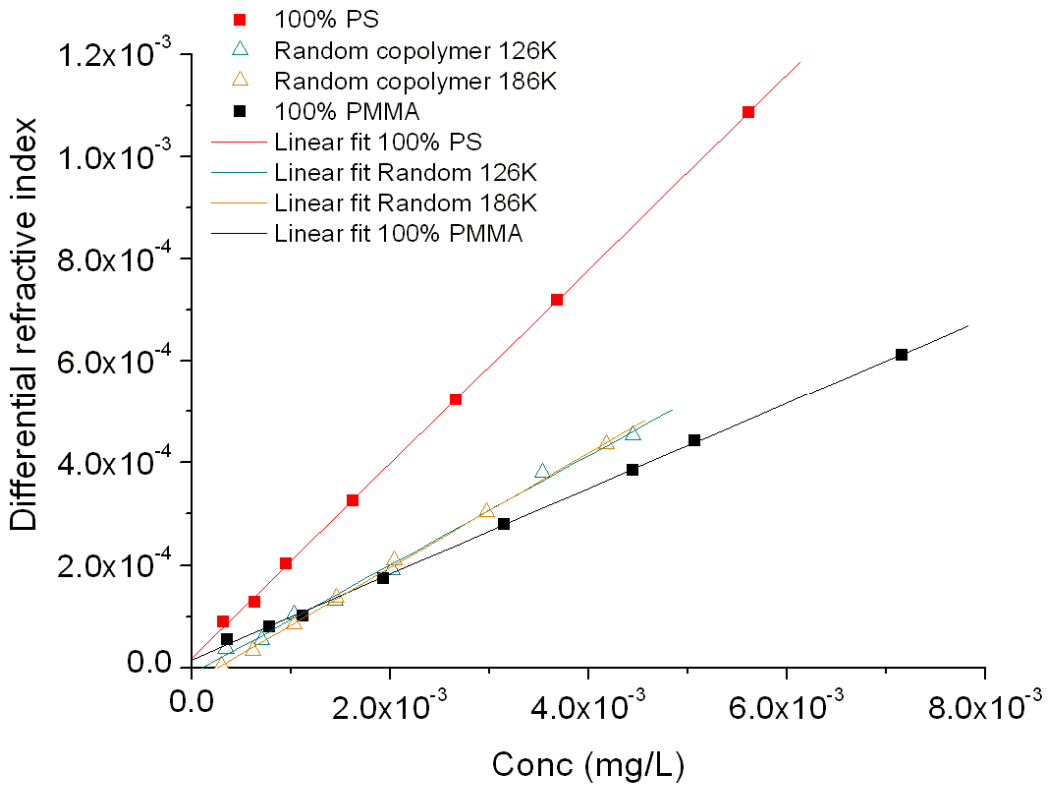

Figure 4.2 - dn/dc of the homopolymer and the random copolymer

Using equation 4.1 or 4.2, the percentage composition of random copolymer can also be calculated. Results are shown in table 4.5.

Table 4.5- calculated and measured dn/dc values of the random copolymers.

Polymer	Mole % of PS*	Calculated dn/dc (mL/g)	Measured dn/dc (mL/g)
PS-*co*-PMMA (Mn 126K)	20%	0.108 ± 4.0	0.108 ± 0.004
PS-*co*-PMMA (Mn 186K)	25%	0.113 ± 2.2	0.111 ± 0.002
* Percentages determined by the manufacturer using ^{1}H-NMR.			

4.1.4 - dn/dc of alternating copolymers

Due to their alternating nature, the composition of the alternating copolymers is expected to be 50% of each monomer. This can be concluded from the dn/dc values of the two alternating copolymers being the same and from the general shape of the dn/dc plot in figure 4.3, where the dn/dc trends of the two alternating copolymers overlap at the mid-distance between the two homopolymers.

The percentage composition of the alternating copolymers can be also back-calculated using the same method that was generally derived for the block copolymers, as shown in table 4.6.

Table 4.6- back calculating the % composition of the alternating copolymers

Polymer	dn/dc	Finding the % of PS (X)	Calculated % of PS	% of PS
PS-*alt*-PMMA (Mn 235K)	0.136 ± 0.002	0.136= 0.191X+0.087(1-X)	47.1 ± 2.4	50%
PS-*alt*-PMMA (Mn 561K)	0.137 ± 0.001	0.137= 0.191X+0.087(1-X)	48.1 ± 1.7	50%
* Percentages determined by the manufacturer using ^{1}HNMR.				

Using equation 4.1 and 4.2, the percentage composition of alternating copolymers can be calculated. Results are shown in table 4.7.

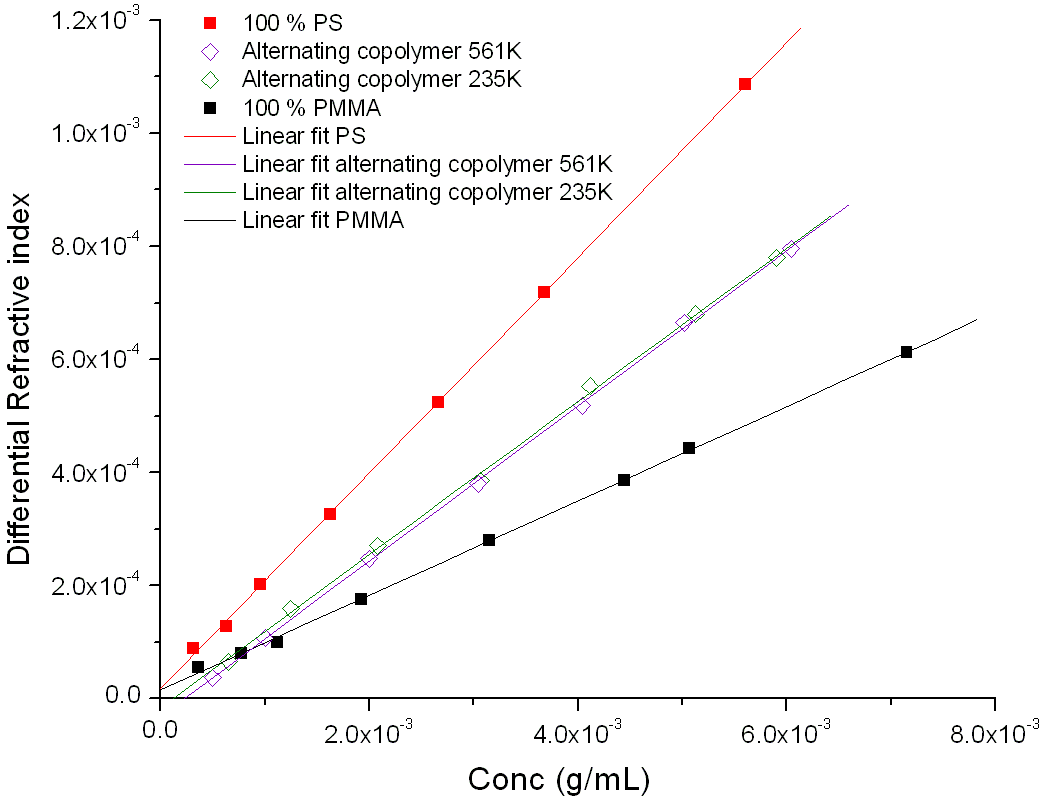

Figure 4.3 - dn/dc of the Homopolymer and the alternating copolymer

Table 4.7- calculated and measured dn/dc values of the alternating copolymers.

Polymer	**Mole % of PS***	**Calculated dn/dc (mL/g)**	**Measured dn/dc (mL/g)**
PS-*alt*-PMMA (Mn 235K)	50%	0.139	0.136 ± 0.002
PS-*alt*-PMMA (Mn 561K)	50%	0.139	0.137 ± 0.001

4.1.5 – Determination of dn/dc values of copolymers:

The dn/dc results obtained for the block, random, and alternating copolymers indicates that the dn/dc is a function of the percentage composition of the copolymers. The plot of

dn/dc versus percentage PS of the different copolymers shows how all copolymers fit the same trend. This fit, shown in figure 4.4, proves that dn/dc property is independent of the monomeric arrangement. From figure 4.4, we obtain the relation ship:

$$dn/dc = (0.0011)\times(\%PS) + 0.00852 \qquad (4.3)$$

which can serve two purposes: 1) To obtain the percentage PS of a PS-PMMA copolymer, if the dn/dc of the copolymer is known and 2) To obtain the dn/dc of a PS-PMMA copolymer if either the percentage PS or percentage PMMA is known. It should be noted that this relationship is specific to copolymers of PS and PMMA, and the dn/dc values are specific to solution in THF at 25°C and for λ_o=585 nm. However, as has been demonstrated, relation 4.3 is independent of random, block, or alternating arrangement of the PS and PMMA units in a copolymer.

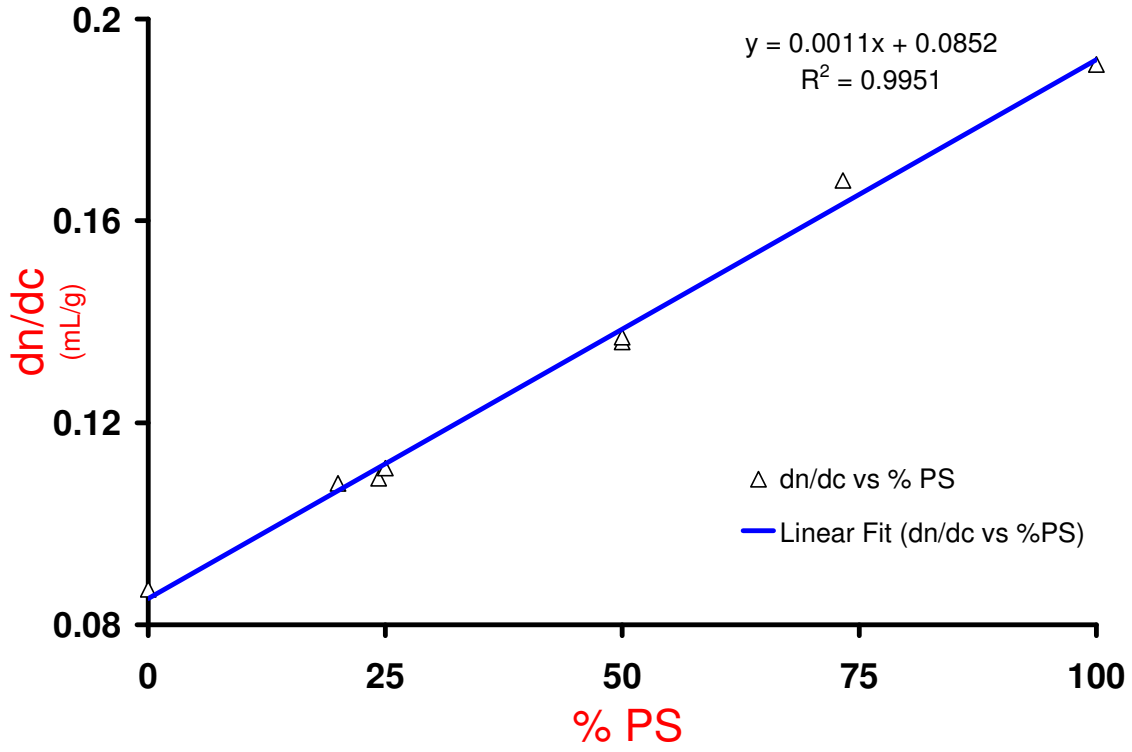

Figure 4.4 - dn/dc vs % PS plot of the data in table 4.8

Table 4.8- mole % of PS and measured dn/dc values of the polymers.

Polymer	**Mole % of PS***	**Calculated mole % of PS**	**Calculated dn/dc (mL/g)**	**Measured dn/dc (mL/g)**
PMMA	0	0 ± 3	0.087	0.087 ± 0.001
PS-*co*-PMMA (Mn 126K)	20	20.2 ± 4	0.108	0.108 ± 0.004
PS-*b*-PMMA (46K, 138K)	24.3	21.2 ± 2.2	0.112	0.109 ± 0.001
PS-*co*-PMMA (Mn 186K)	25	23.1 ± 2.2	0.113	0.111 ± 0.002
PS-*alt*-PMMA (Mn 235K)	50	47.1 ± 2.4	0.139	0.136 ± 0.002
PS-*alt*-PMMA (Mn 561K)	50	48.1 ± 1.7	0.139	0.137 ± 0.001
PS-*b*-PMMA (131K, 46K)	73.3	77.9 ± 2.2	0.163	0.168 ± 0.001
PS	100	100 ± 3	0.191	0.191 ± 0.002
* percentages obtained form the manufacturer				

The percentage composition of the copolymers is determined using an equation relating the dn/dc value of the copolymer to the dn/dc values of the corresponding homopolymers. The equation used for determining the composition of the copolymers is originally derived for the block copolymers, but in this project we successfully extended using this equation to find the composition of the other copolymers as shown in table 4.8.

4.2 – Second virial coefficient (A_2) Results

The second virial coefficient (A_2) is a parameter used to define the thermodynamic state of a polymer solution. The sign of the second virial coefficient, at a certain temperature and in a given solvent, corresponds to how well a polymer is solvated under these

conditions. In general, three different thermodynamic states of a polymer are defined through the second virial coefficient: 1) The ideal state, i.e. theta state, where the second virial coefficient is zero. At this state, a linear polymer is neither expanded nor contracted when compared to its size in melt. 2) The state when the second virial coefficient is positive, corresponding to polymer being well-solvated. At this state, the solvent is called a good solvent and the size of the polymer is more extended than its size in melt. 3) The state corresponding to the polymer being poorly solvated corresponds to the second virial coefficient being negative. At this state, the solvent is called a poor solvent with the polymer is less extended than in the melt. The A_2 values of the homopolymers and copolymers we studied are determined from off-line MALS, as described in section 3.4 and as shown in table 4.9.

Table 4.9- A_2 values for the polymers studied in THF at 25°C

Polymer	**A_2 (mol mL/g^2)**
PS (49K)	$(7.36 \pm 0.07) \times 10^{-04}$
PS (133K)	$(6.43 \pm 0.04) \times 10^{-04}$
PMMA (53K)	$(4.35 \pm 0.29) \times 10^{-04}$
PMMA (138K)	$(4.72 \pm 1.02) \times 10^{-04}$
PS-*b*-PMMA (46K, 138K)	$(3.26 \pm 0.05) \times 10^{-04}$
PS-*b*-PMMA (131K, 46K)	$(5.45 \pm 0.03) \times 10^{-04}$
PS-*co*-PMMA (Mn 126K)	$(6.08 \pm 0.09) \times 10^{-04}$
PS-*co*-PMMA (Mn 186K)	$(4.56 \pm 0.04) \times 10^{-04}$
PS-*alt*-PMMA (Mn 235K)	$(5.40 \pm 0.09) \times 10^{-04}$
PS-*alt*-PMMA (Mn 561K)	$(5.39 \pm 0.11) \times 10^{-04}$

The second virial coefficient depends on several parameters. These parameters are: 1) The molar mass and the degree of polymerization of the polymer. 2) Bond length of the monomers. 3) The Flory Huggins parameter (χ) of the polymer. The relation

between the second virial coefficient and the different parameters is explained in the following equations[52].

$$A_2 = \left(\frac{N_A}{2m^2}\right)\beta h(\bar{Z}) \qquad (4.4)$$

$$\beta = 2\left(\frac{V_1}{N_A}\right)\left(\frac{1}{2} - \chi\right) \qquad (4.5)$$

$$h(\bar{Z}) = \frac{[1-(1+0.683\bar{Z})^{-7.39}]}{5.047\bar{Z}} \qquad (4.6)$$

$$\bar{Z} = \frac{Z}{(1+1.779Z)} \qquad (4.7)$$

$$Z = (\frac{3}{2\pi})^{\frac{3}{2}}(\frac{\beta}{a^3})n^{\frac{1}{2}} \qquad (4.8)$$

N_A is Avogadro's number, m the molar mass of a chain segment, β is the binary cluster integral between segments, V_1 is the molar volume of the solvent, χ is the Flory Huggins interaction parameter, $\bar{Z}$ is the effective excluded volume parameter, Z is the excluded volume parameter, a is the effective bond length, and n is the number of segments in a polymeric molecule.

For small values of Z, i.e. for low molar mass polymers, the effective excluded volume ($\bar{Z}$) becomes negligible. For small values of $\bar{Z}$, the function $h(\bar{Z})$ is a decreasing function of $\bar{Z}$, with $h(\bar{Z})$ approaching one for Z=0. The second virial coefficient of the polymer is directly proportional to the function $h(\bar{Z})$ ($A_2 \propto h(\bar{Z})$) , therefore, the second virial coefficient for low molar mass polymers is expected to decrease with increasing the polymer's molar mass ($A_2 \propto M^{-1}$, for small M).[52]

For large values of Z, i.e. for high molar mass polymers, the function $h(\bar{Z})$ becomes a constant, given by equation (4.9). Thus, high molar mass polymers the second virial coefficient is constant and independent of molar mass (A_2 = C, where C = constant for large M).[52]

$$\lim_{\bar{Z}\to\infty} h(\bar{Z}) = 0.320 \qquad (4.9)$$

4.2.1 - A_2 values of homopolymers

From the results shown in table 4.9, it can be seen that the second virial coefficients for the same homopolymer (PS or PMMA) show a decrease with increasing the molar mass. This is due to the fact that A_2 is inversely proportional to the molar mass of a linear polymer, where A_2 is expected to decrease quickly for small molar masses and then asymptotically for large molar masses. The range where A_2 starts decreasing asymptotically with molar mass depends on the chemistry of the polymer and the solvent/ temperature conditions[53].

Another conclusion about the thermodynamic state of the PS and PMMA can be deduced when comparing the A_2 values of the PS and PMMA. The A_2 values for PS are higher than those of PMMA having the same molar mass. This indicates that the PS is better solvated than PMMA in THF at 25°C.

A_2 of the random copolymers: The A_2 values of the two random copolymers can be compared to each other because the two random copolymers have nearly the same percentage chemical composition. The 186K random copolymer has a lower A_2 value than the 126K copolymer, due to the second virial coefficient and the molar mass being inversely related for low molar mass polymers.

A_2 of the alternating copolymers: For the alternating copolymers, it can be observed that the A_2 values are the same even though the two alternating copolymers have vastly different molar mass. This is because the function $h(\bar{Z})$ reaches a plateau for high molar mass polymers, as explained in section 4.2.

A_2 of the block copolymers: The block copolymers have a different percentage chemical composition but approximately the same molar mass as the other block copolymer. Thus, the effect of the percentage composition on A_2 can be studied in block copolymers, independently of molar mass effects. The block copolymer richer in polystyrene has an A_2 value larger than the A_2 of the copolymer richer in PMMA. We relate this to the off-line MALS measured. A_2 values for PS and PMMA homopolymers, where it was found that THF is a better solvent for PS than for PMMA at the given experimental conditions. As indicated by $(A_2^{PS})_M > (A_2^{PMMA})_M$ where the subscript M indicates values for the same molar mass.

4.3 - Molar mass determination:

A synthetic polymer sample contains molecules with different degrees of polymerization, which originates from the polymerization process itself. The polydispersity index (PD) value can be used to measure the breadth of the molar mass distribution. A monodisperse polymer is a polymer characterized by a narrow distribution of molar masses and a PD value close to one. On the other hand, a polydisperse polymer corresponds to a polymer with broad molar mass distribution and PD larger than one. From the polydispersity indices in table 4.10, the homopolymers and the block copolymers are expected to have narrow molar mass distributions, while alternating and random copolymers are expected to have broad MMDs.

PD values are poor indicatives of the shape and breadth of molar mass distributions. Moreover, the PD is incapable of showing the fraction of each molar mass within a sample. Complete knowledge of the MMD and individual molar masses are obtained from the online SEC/MALS/VISC/DRI experiments. Shown in figure (4.4) are the MMD of a block and alternating copolymer of PS and PMMA

Table 4.10 - Mw and polydispersities of the polymers

Polymer	PD[a] M_w/M_n	M_w[a] (g/mol)
PS (49K)	1.01 ± 0.00	$(4.55 \pm 0.23) \times 10^4$
PS (133K)	1.01 ± 0.01	$(1.13 \pm 0.00) \times 10^5$
PMMA (53K)	1.02 ± 0.01	$(5.38 \pm 0.01) \times 10^4$
PMMA (138K)	1.03 ± 0.04	$(1.30 \pm 0.02) \times 10^5$
PS-*b*-PMMA (46K, 138K)	1.06 ± 0.01	$(2.20 \pm 0.04) \times 10^5$
PS-*b*-PMMA (131K, 46K)	1.02 ± 0.00	$(1.82 \pm 0.01) \times 10^5$
PS-*co*-PMMA (Mn 126K)	1.39 ± 0.08	$(2.13 \pm 0.09) \times 10^5$
PS-*co*-PMMA (Mn 186K)	1.43 ± 0.03	$(2.48 \pm 0.02) \times 10^5$
PS-*alt*-PMMA (Mn 235K)	1.44 ± 0.03	$(3.11 \pm 0.02) \times 10^5$
PS-*alt*-PMMA (Mn 561K)	1.33 ± 0.08	$(8.72 \pm 0.44) \times 10^5$
[a] Values from SEC/MALS/DRI/VISC online experiments		

The molar mass distribution curves for polydisperse and monodisperse polymers are different in their range covered, as well as in each individual molar mass. Figure 4.5 compares the MMD of a narrow polydispersity block copolymer with that of a wide polydispersity alternating polymer.

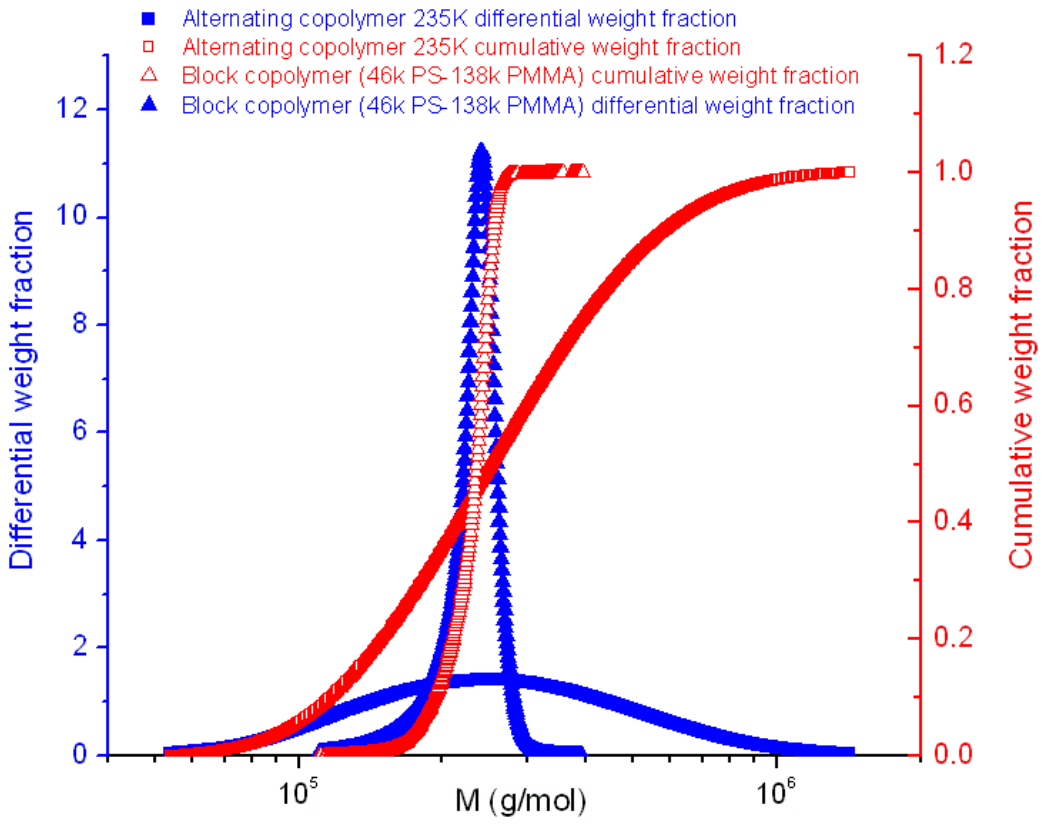

Figure 4.5 – molar mass distribution of a block and an alternating copolymer

The alternating and the random copolymers are polydisperse polymers as shown in table (4.7). As a result, the MMD plots of these copolymers are expected to cover a wide molar mass range. As shown in figure 4.6, the continuous distribution of the molar mass plots covers more than a degree of magnitude. These plots are informative of: 1) The range of molar mass covered by the sample. 2) The fraction of each individual molar mass within the sample. 3) The estimate of the molar mass moments (Mw, Mn, Mz). 4) The understanding of some properties related to the molar mass ranges covered along with the fraction of the individual molar masses, examples include: viscosity, toughness, heat resistance, tensile strength, as well as rheological properties.[54]

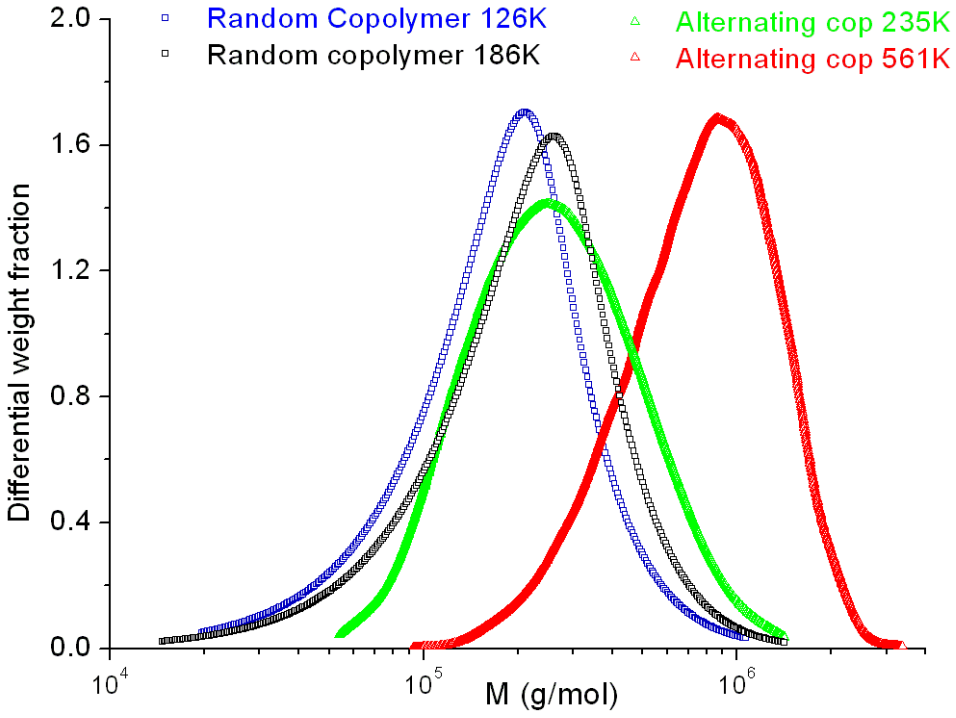

Figure 4.6 – molar mass distribution of the random and alternating copolymers

4.4 - Intrinsic viscosity [η]data

The intrinsic viscosity, [η], is calculated from the ratio of the signal from the differential viscometer to the signal from the differential refractometer for very dilute solutions. This ratio is equivalent to the ratio of the specific viscosity to the concentration at infinitely dilute concentrations, as expressed in equation 4.10.

$$[\eta] = \lim_{c \to 0} \frac{\text{Visc Signal}}{\text{DRI Signal}} = \lim_{c \to 0} \frac{\eta_{sp}}{C} \qquad (4.10)$$

The intrinsic viscosity is dependent on the molar mass of the polymer is structure in solution. This relation between intrinsic viscosity and molar mass is expressed by the Mark-Houwink:

$$[\eta] = K \times M^{a} \qquad (4.11)$$

Where *a* is the slope of the plot log [η] vs log M. This slope *a* depends on the conformation of the polymer in the solution and on the thermodynamics of the dilute polymer solution.

4.4.1 - Intrinsic viscosities of the homopolymers

Table 4.11 – intrinsic viscosities of the homopolymers

Polymer	**[η]*** (mL/g)
PS (49K)	29.5 ± 0.1
PS (133K)	60.1 ± 0.6
PMMA (53K)	21.4 ± 0.6
PMMA (138K)	46.3 ± 0.9
* Determined from SEC/MALS/VISC/DRI online experiments	

When comparing the intrinsic viscosities of the homopolymers, we notice that the intrinsic viscosities of PS and PMMA of approximately the same M are considerably different from each other. PS has a higher intrinsic viscosity than PMMA of almost identical M, which indicates that PS is more extended in solution. This agrees with the A_2 results indicating that THF is a better solvent for PS than for PMMA of the same M.

4.4.2 - Intrinsic viscosities of the block copolymers

We compare the intrinsic viscosities of the block copolymers to the intrinsic viscosities of the corresponding homopolymers. To this effect, we chose homopolymers of PS and PMMA of the same M as the corresponding PS and PMMA blocks in the block copolymers. The intrinsic viscosity of a block copolymer is seen to be the sum of the intrinsic viscosities of the two homopolymers with molar masses representing the molar

masses of the individual blocks in the block copolymer. This additive relationship is a result of the two blocks in a block copolymer being joined at a single point. Thus, the two blocks behave independently of each other and the [η] of the block copolymer, as a whole, is the sum of the [η]s of the two blocks. The negligible interaction between dissimilar segments, which occurs at the only junction point between blocks, does not affect the [η] of the block copolymers within the limits of the experimental measurements.

Table 4.12 – intrinsic viscosities of the block copolymers

Polymer	**[η]*** (mL/g)	**Polymer**	**[η]*** (mL/g)
PS (49K)	29.5 ± 0.1	PS (133K)	60.1 ± 0.6
PMMA (138K)	46.3 ± 0.9	PMMA (53K)	21.4 ± 0.6
PS-*b*-PMMA (46K, 138K)	67.5 ± 1.2	PS-*b*-PMMA (131K, 46K)	76.5 ± 0.9
* Determined from SEC/MALS/VISC/DRI online experiments			

Furthermore, even though the two block copolymers have comparable molar masses, the intrinsic viscosity of the block copolymer richer in PS is higher than the [η] of the block copolymer richer in PMMA. This is due to the fact that PS is better solvated than PMMA in THF. Thus the block copolymer richer in PS will occupy a larger hydrodynamic volume in solution and its intrinsic viscosity will be larger than the [η] of the block copolymer poorer in PS.

4.4.2 - Intrinsic viscosities of random and alternating copolymers

When comparing the intrinsic viscosities of the two random copolymers we notice that the intrinsic viscosities of the two are considerably different from each other. The 186K random copolymer has a higher intrinsic viscosity than the 126K random copolymer,

even though their percentage composition is similar. This difference is due to the difference in the molar masses of the random copolymers, as indicated by the Mark-Houwink equation, equation (4.11). Intrinsic viscosity is expected to increase proportionally with M, a relation which applies to both the random and alternating copolymers examined, given their constancy in chemical composition.

Table 4.13 – intrinsic viscosities of the random and alternating copolymers

Polymer	**[η]*** (mL/g)
PS-*co*-PMMA (Mn 126K)	77.4 ± 1.9
PS-*co*-PMMA (Mn 186K)	86.6 ± 1.3
PS-*alt*-PMMA (Mn 235K)	90.9 ± 2.5
PS-*alt*-PMMA (Mn 561K)	239.9 ± 3.0
* Determined from SEC/MALS/VISC/DRI online experiments	

4.5 - Mark-Houwink slopes

The slope, a, of the Mark-Houwink plot of the log[η] versus log M helps in identifying the shape of the polymer in solution. The table below relates the shape of generic polymers to their structure in solution[55]

Table 4.14 - Mark-Houwink slopes of the different shapes in solutions [55]

Polymer shape	**Mark-Houwink slope (a)**
Sphere	0
Unperturbed coil	0.5
Rigid rod	2
Linear random coils in good solvent/T° conditions	0.65-0.8

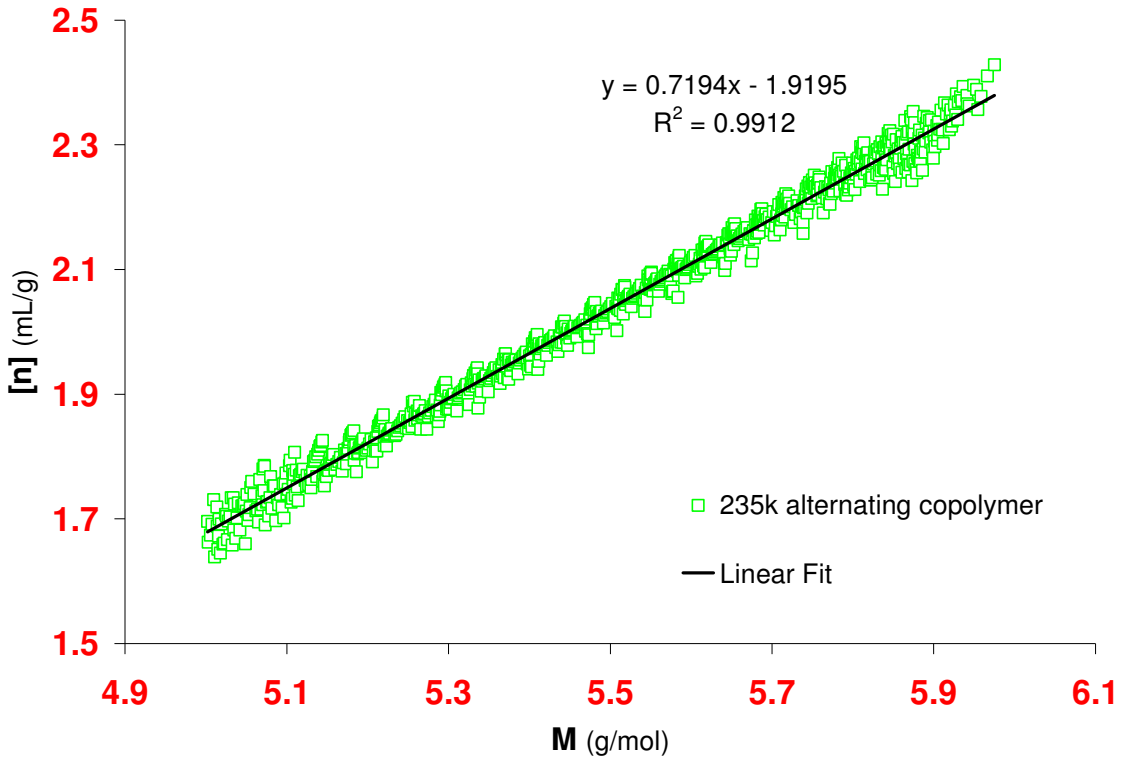

Figure 4.7 – Mark-Houwink plot of alternating copolymer 235K

From the Mark-Houwink slopes in table 4.15 we can conclude that the alternating copolymers and the random copolymers behave as linear random coil at good solvent/temperature conditions. Mark-Houwink plots of the block copolymers cannot be obtained via this method, due to the extremely narrow polydispersity of these copolymers. It can be expected, from our previous discussion about the relation between the intrinsic viscosity of block copolymers and that of the corresponding the homopolymer blocks, that the block copolymers have the same random coil structure in solution as the homopolymers.

Table 4.15 – Mark-Houwink slopes of alternating and random copolymers

Polymer used	**Mark-Houwink Slope**
PS	0.71[a]
PMMA	0.72[a]
PS-*co*-PMMA (Mn 126K)	0.72 ± 0.02 [b]
PS-*co*-PMMA (Mn 186K)	0.70 ± 0.01 [b]
PS-*alt*-PMMA (Mn 235K)	0.72 ± 0.00 [b]
PS-*alt*-PMMA (Mn 561K)	0.78 ± 0.00 [b]
[a] Values averaged from data obtained from the Polymer Handbook under the same solvent/Temperature conditions[56]	
[b] Determined from SEC/MALS/VISC/DRI online experiments	

In this section we determined the intrinsic viscosity values of the polymers and the Mark-Houwink slopes of the polydisperse polymers. The intrinsic viscosity values are important for determining many physical properties as such molar mass and viscometric radius. Intrinsic viscosities of polydisperse polymers are also used for determination of the structure of the polymers in solution. The determination of the structure of polymers in solution is determined using Mark-Houwink plots of the intrinsic viscosities versus the molar mass.

4.6- Radius of gyration (Rg)

The radius of gyration, the root mean square distance of the polymer repeat units from their common center of mass, is determined from the angular dependence of the intensity of the scattered light via MALS. For samples with Rg values smaller than ~ 10 nm, there is no angular dependence on the intensity of the scattered light via MALS at typical laser wavelengths and in most “typical” solvents. Due to this limitation, we were unable to determine the Rg values for the homopolymers used. The Rg values of the copolymers are determined from the SEC/MALS/VISC/DRI online experiments and with results given in table 4.15.

The Rg values of the block copolymers are close to each other in size due to two competing effects: Molar mass and percentage composition. The block copolymer richest in PMMA is also higher in mass, as shown in table 4.10, and therefore might be expected to be of larger size than the PS rich block copolymer. The step length of the PMMA and PS monomers are shown in table 4.17.

In the case of the block copolymer richest in PS, the abundance of the PMMA is less, therefore expected to be bigger in size but shortened by its smaller molar mass.

Table 4.16 – Rg values of the block copolymers

Polymer	**Rg[a] (nm)**
PS-*b*-PMMA (46K, 138K)	(16 ± 0) nm
PS-*b*-PMMA (131K, 46K)	(15 ± 0) nm
PS-*co*-PMMA (Mn 126K)	(19 ± 0) nm
PS-*co*-PMMA (Mn 186K)	(23 ± 0) nm
PS-*alt*-PMMA (Mn 235K)	(35 ± 0) nm
PS-*alt*-PMMA (Mn 561K)	(57 ± 0) nm
[a] Values from SEC/MALS/VISC/DRI online experiments	

Table 4.17 – Step lengths of styrene and methyl methacrylate

Monomer	Step length (nm)[57]
S	0.530
MMA	0.481

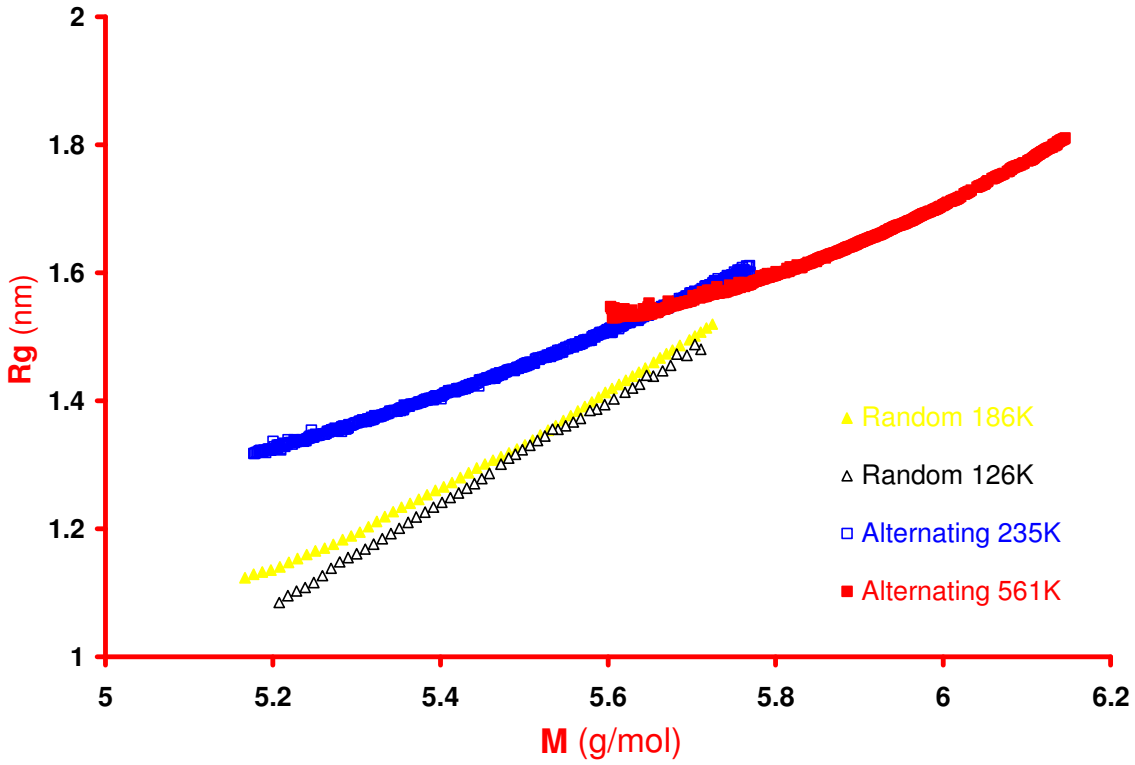

Figure 4.8 – Rg vs M for the random and alternating copolymers on a log scale

In figure 4.8, we notice that the Rg values of the random copolymers are lower than the Rg values of the alternating copolymers of the same M. This is due to two factors: First, for the same M_w, the alternating copolymers are richer than the random copolymers in PS than in PMMA. Thus, the alternating copolymer is expected to be larger in solution than the random copolymer. Second is the presence of intrachain repulsion between S and MMA. An alternating sequence of the monomers within the chain results in maximum intrachain repulsion and a more extended structure in solution. As can be seen, both the relative chemical composition and the monomeric sequence of the alternating copolymers, as compared to the random copolymers, contribute to the more extended structure in solution of the former as compared to the latter[11].

The slopes of the conformation plots of log R_g versus log M in figure 4.8 are indicative of the structure of the polymers in solution. In section 4.5, we determined the structure of the alternating and the random copolymers to be random coil. As a result, the

slopes of the conformation plots of the alternating and random copolymers are expected to be close to 0.5, which is the value for a random coil structure in solution.[43, 58]

Table 4.18 – Mark-Houwink slopes and conformation slopes for alternating and random copolymers

Polymer used	**Mark-Houwink slope***	**Conformation plot slope***
PS-*co*-PMMA (Mn 126K)	0.72 ± 0.02	0.80 ± 0.03
PS-*co*-PMMA (Mn 186K)	0.70 ± 0.01	0.72 ± 0.06
PS-*alt*-PMMA (Mn 235K)	0.72 ± 0.00	0.49 ± 0.00
PS-*alt*-PMMA (Mn 561K)	0.78 ± 0.00	0.53 ± 0.00
* Determined from SEC/MALS/VISC/DRI online experiments		

The slopes of the Mark-Houwink and the conformation plots of the alternating and the random copolymers are shown in table 4.18. The slopes of the two types of plots for the alternating copolymers are in agreement with each other regarding the structures of these copolymers in solution. This indicates that the alternating copolymers are random coil in solution and that the 561K alternating copolymer is slightly more extended than the 235K alternating copolymer.

For random copolymers, the slopes of the conformation plots fall between the random coil and the rigid rod values, 0.5 for the former and 1 for the latter. This result is in contradiction with the results obtained from the Mark-Houwink plots indicating that these random copolymers adopt random coil structures in solution. To further explain, figure 4.8 is a good visual aid to understand the increase in the slopes of the conformation plots of the random copolymers. In this figure, dotted lines correspond to conformation plots of random coil homopolymers with slightly different degrees of extension increasing with increasing curve number. I.e., curve one denotes a minimally extended random coil homopolymer and curve five a maximally extended random coil homopolymer. Other experiments in our lab have shown that polydisperse random

copolymers adopt an increased extended structure as a function of molar mass. As a result of the increase in the degree of extension with the increase in molar mass, random copolymers would fit on different lines identified by dots connecting them as shown in figure 4.9. The bold line connecting these dots reflects the increase in the slope of the conformation plot of the random copolymer.

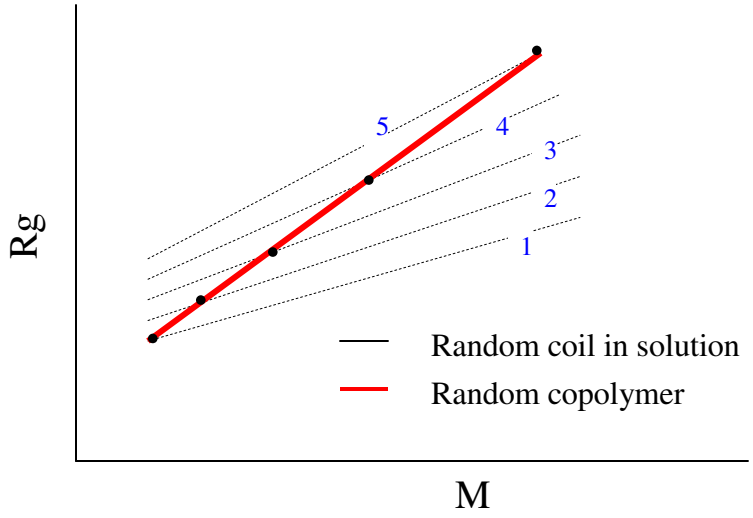

Figure 4.9 – Conformation plots of the random coil structures in solution

In this section we determined the Rg values and the conformation plot slopes of the copolymers. Knowledge of the radius of gyration is essential for many reasons: For determining physical structural such as fractal dimension; dimensionless radii ratios (R_η/R_g and R_g/R_h); to specify the structure of the polymer using the conformation plots; and to determine the molar mass of the polymer using the conformation plots equation.

CHAPTER FIVE

CONCLUSIONS

In this project, we studied the dilute solution properties of PS and PMMA homopolymers and alternating, block and random copolymers of these homopolymers. The dilute solution was the medium of choice because of the ease to work in this medium added to the ability to obtain a wealth of information about polymers in dilute solution via a multi-detector SEC approach. The dilute solution properties were studied using size-exclusion chromatography (SEC) coupled to multi-angle light scattering (MALS), viscometry, and refractometry detectors. Using this triple-detector SEC setup, we successfully determined important properties of the polymers and copolymers such as: 1) Differential refractive index increments. 2) Second virial coefficients. 3) Molar mass and molar mass distributions. 4) Intrinsic Viscosities. 5) Radii of gyration. 6) Relations between $[\eta]$ or R_g and M. Each of the obtained properties is important for knowledge about the polymer, as explained below.

From the offline DRI experiments, we obtained the specific refractive index increment (dn/dc) values of the copolymers and the corresponding homopolymers. Consequently, we determined the bulk percentage composition of copolymers using dn/dc, by relating the dn/dc of the copolymers to the dn/dc of the corresponding homopolymers. The method we used for determining the composition of the copolymers was originally derived for the block copolymers, but in this project we successfully extended using this equation to calculate the composition of alternating and random copolymers. The dn/dc value can also be used for determining other properties such as: 1) The concentration of polymer in solution using the refractive index of the solution. 2) The refractive index of solution using the concentration of the polymer in solution. 3) Molar mass and size via static light scattering experiments.

The second virial coefficient, A_2, was determined from off-line MALS experiments. From this parameter, we were able to conclude that THF is a good solvent

for both PS and PMMA and for the corresponding copolymers of these homopolymers. We were also able to determine that THF is a better solvent for PS than for PMMA. We then used the A_2 values of copolymers of similar molar mass as a criterion to compare their percentage composition. Moreover, the relation between the molar mass and the second virial coefficient was shown. The second virial coefficient is not only important for determining the thermodynamic state of the solution, but also in determining other properties as such the thermodynamic radius.

The molar mass, the polydispersity indices, as well as the molar mass distributions of the polydisperse copolymers were obtained from the online SEC/MALS experiments. Knowledge of the molar mass and the molar mass distribution is important because these affect the polymer properties such as viscosity, toughness, resistance to heat, and other rheological properties. Molar mass is also used for determining other properties such as: 1) Structural properties as M is most used to calculate R_g, thermodynamic radius, viscometric radius and fractal dimension. 2) Conformation of the polymer in solution using conformation or Mark-Houwink plots. 3) Intrinsic viscosity.

The intrinsic viscosity was determined from the online triple-detector SEC set-up. The intrinsic viscosity of the block copolymers, as compared to that of the individual homopolymer blocks, showed that the two blocks within the block copolymer are independent of each other and that negligible intrachain interaction is present at the only junction point between blocks present in block copolymers. Mark-Houwink plots were also used to determine that the copolymers and the homopolymers have a random coil structure in THF. Also, the intrinsic viscosity is important for determining other properties such as molar mass, viscometric radius, and the polymer draining function.

Finally, the radius of gyration of the copolymers was determined for online SEC/MALS experiments. The radius of gyration of a polymer is important for determining the size of the polymer, as well as the structure in solution, using conformation plots of Rg versus molar mass. The structure of the polymer in solution can be also determined using other methods such as dimensionless radii ratios (R_η/R_g and

R_g/R_h), and fractal dimensions. Finally, the molar mass of the polymer can be determined from the radius of gyration if the conformation plot equations are known.

APPENDIX

UNDERSTANDING OF THE CONCEPT OF NEGATIVE RADII IN POLYMERIC SOLUTIONS

Overview

The purpose of this project is to give a better understanding of the concept "size of a polymer". Usually, this term is recognized as the root mean square distance of the monomers from their common center of mass, as denoted by the radius of gyration (R_g). Actually, there are four different ways to define the size of a polymer in solution; each of these definitions based on a specific macromolecular radius. The molecular radii related to the size of the polymer in solution are the radius of gyration (R_g), the viscometric radius (R_η), the thermodynamic radius (R_T), and the hydrodynamic radius (R_H)[5,59-61].

The radius of gyration (R_g) is a statistical radius as well as the only nonequivalent-hard-sphere radius used to define the size of a polymer in solution. This radius is determined via static multi-angle light scattering and it depends on the difference in the intensity of the scattered light measured at dissimilar angles. The radius of gyration of the polymer is defined as per[5,55,59-61].

$$R_G = \sqrt{\frac{\sum_i^N (r_i - R_{cm})^2}{N}}$$

Where N is the number of monomers in a polymeric chain, r_i is the location of the ith monomer, and R_{cm} is the location of the center of mass.

The viscometric radius (R_η) is the second method of understanding the size of a polymer in solution. R_η is defined as the radius of a hard sphere that enhances the viscosity of the solvent by the same amount imparted by the polymer. This radius is calculated using a equation relating the intrinsic viscosity [η] to the molar mass M of a

polymer. Thus, both static light scattering and differential viscometry techniques are needed to obtain this radius. The equation for calculating the viscometric radius is:[5,59,60]

$$R_\eta \equiv \left(\frac{3\,[\eta]\,M}{10\,\pi\,N_A} \right)^{1/3}$$

Where N_A is Avogadro's number.

The hydrodynamic radius (R_H) is another means of measuring the size of a polymer in solution. R_H is identified as the radius of a hard-sphere that diffuses at the same velocity as does the polymer. R_H is usually determined using techniques capable of measuring the translational diffusion coefficient D_T of the polymer in solution. An example of such a technique is dynamic light scattering (DLS). Below, is the equation of the hydrodynamic radius[5,46,59].

$$R_H = \frac{k_B T}{6\pi\eta_s D_T}$$

Where k_B is Boltzmann's constant, T is the absolute temperature (in Kelvin), η_s is the viscosity of solvent, and D_T is the translational diffusion coefficient.

The last method of determining the size of the polymer in solution is by using the thermodynamic radius (R_T). This radius represents the radius of a sphere whose volume is equivalent to the excluded volume of a polymer. The excluded volume is defined as the difference in the volume of the polymer occupied at a certain solvent/temperature condition compared with the volume occupied under ideal conditions. The ideal state of a polymer, i.e. the theta state, is the state where the change in Gibbs free energy of a solution is equal to zero. The thermodynamic of the viscometric radius is dependent on the second virial coefficient A_2 and the weight-average molar mass M_W according to [5,52,55,57,60].

$$R_T \equiv \left(\frac{3\,A_2\,M_w^2}{16\,\pi\,N_A} \right)^{1/3}$$

RT is determined using static, off-line MALS, a technique which yields both A_2 and M_w.

This study contributes to the understanding of the size of polymers by comparing the different polymeric radii, as well as introducing the concept of negative radii values. To accomplish these goals, we choose to work at solvent / temperature conditions very close to the theta state of the polymer. At this state, the effects we are trying to measure are more pronounced than of any other solvent/temperature conditions. This better manifestation is related to the specific properties of the theta state, as will be explained below[5,59,60].

At the specific solvent/temperature conditions of the theta state, the size of a linear polymer in solution is neither extended nor contracted with respect to its size in melt. As a result, the excluded volume as well as the second virial coefficient under these conditions is equal to zero. Consequently at θ conditions, the R_T value of the polymer is equal to zero in contrast to the values of the other radii which can be expected to be non-zero. At solvent/temperature conditions slightly less thermodynamically favorable than theta state, the size of the polymer in solution becomes smaller than in melt. Accordingly, the excluded volume and the second virial coefficient of the polymer become negative resulting in negative, values for the thermodynamic radius[59, 62].

In this project, we provide experimental values supporting the concept of the negative size in polymers. To our knowledge, these experimental evidences are the first in the literature. We hope that this project enhances the understanding of the concept of polymer size, as well as illustrates the difference between the different polymeric radii[1].

Experimental

Materials

Polystyrene (PS) and poly(methyl methacrylate) (PMMA) narrow polydispersity linear standards were obtained from Polymer Laboratories, cyclohexane and acetonitrile from

Fischer Scientific, and *n*-butyl chloride from EMD. All materials were used as received, without further purification.

Multi-angle light scattering (MALS)

The second virial coefficients (A_2) of PS and PMMA at the appropriate solvent/temperature conditions were measured by performing off-line MALS experiments in which a series of seven sample dissolutions, ranging from 0.5-5.0 mg/mL, were injected directly into the light scattering photometer, a Wyatt Dawn EOS with Peltier-driven temperature regulation of the read head, using a Razel model A-99EJ syringe pump. Flow rate was 0.1 mL/min. Sample solutions were filtered through 0.2 μm Teflon syringe filters, neat solvent for baseline determination through a 0.02 μm Teflon syringe filter. Normalization of the photodiodes of the MALS unit was performed using either a 7000 g/mol narrow polydispersity linear PS standard (M_w/M_n = 1.04) or a 7800 g/mol narrow polydispersity linear PMMA standard (M_w/M_n < 1.14). Data acquisition and processing were done with Wyatt's ASTRA V software (V. 5.1.9.1). Plotting of the data was performed using the graphical procedure of Zimm, with the data fitted by a first-order polynomial.

Dynamic light scattering (DLS)

As the Wyatt QELS and Dawn EOS MALS units are housed in the same apparatus, determination of the translational diffusion coefficient (D_T) of the polymers, from whence the hydrodynamic radii (R_H) are derived, was performed in a similar fashion to the determination of A_2 described above. While only one concentration of each sample is needed for this type of DLS analysis, we checked our results using several concentrations of each sample and note that virtually identical results were obtained at the different concentrations.

Specific refractive index increment (dn/dc) determination

The specific refractive index increment (d*n*/d*c*) of PS in cyclohexane was determined as 0.131 mL/g, that of PMMA in acetonitrile as 0.130 mL/g, and that of PMMA in *n*-butyl chloride as 0.099 mL/g. The variation in d*n*/d*c* with temperature over the temperature ranges examined was negligible. Determinations were done by injecting seven dissolutions of each sample, ranging from 0.5-5.0 mg/mL, directly into a Wyatt Optilab rEX differential refractometer using the Razel syringe pump. Flow rate was 0.1 mL/min. Sample solutions were filtered through 0.2 μm Teflon syringe filters, neat solvent for baseline determination through a 0.02 μm Teflon syringe filter. The radiation from the light source of the refractometer is filtered to match the vacuum wavelength (685 nm) of the laser in the MALS/DLS unit. Data acquisition and processing were done with Wyatt's ASTRA V software (V. 5.1.9.1).

Results and discussions

The results obtained in this study are summarized in table 1, these results include the second virial coefficient A_2 and the four different radii of specific polymers at certain solvent/temperature conditions. The R_T values were calculated using the second virial coefficient measured in our lab and the molar mass obtained from manufacturer. Accordingly, the sign of second virial coefficient is reflected in the sign of the R_T values and thus positive, negative, and zero values were obtained. The exact theta state was obtained in only one case, namely for PS 189K in cyclohexane, where the second virial coefficient shows a value of zero. For the other polymers under different solvent/temperature conditions, the R_T values fluctuated near zero in either the positive or negative direction. From these results, we can observe negative values of the thermodynamic radius, contrary to the other radii (R_G, R_η, and R_H), which show positive values independent of that of the R_T.

The sensitivity of the theta state to small fluctuations in temperature and, as a result, the difficulty in attaining this state is explained by the data shown in table 1. For 66.5K PS in cylcohexane, the data show that the theta state is between 28 ^oC and 32 ^oC and the small fluctuation in temperature changes the thermodynamic state of the solvent

from a poor solvent to a good solvent. This effect of temperature on the thermodynamic state is more pronounced for the 177.8K PMMA in acetonitrile, where a change in temperature by less than one degree results in changing the thermodynamic state of the solution from slightly good to slightly poor.

Using the data from table 1, the effect of parameters such as molar mass polymer and temperature on the solvation of the polymer can be observed. The increase in the temperature of the solution results in enhancing the solvation of the polymer, expressed as an increase in the second virial coefficient. This can be noticed for the 66.5K PS in cyclohexane and the 177.8K PMMA in acetonitrile at the different temperatures examined. The effect of molar mass on the thermodynamics of the solution can also be deduced when comparing the 68K PS and the 189K PS in cyclohexane at 34 ^{o}C, as well as when comparing the 142.2K PMMA and the 177.8K PMMA in acetonitrile at 29 ^{o}C. In both cases, the increase in molar mass leads to a decrease in the second virial coefficient and, consequently, a decrease in the R_T.

Molar mass and temperature can act as two competing parameters when studying their effect on the second virial coefficient. The increase in the second virial coefficient expected due to an increase in temperature can be compensated for due to an increase in molar mass. As a result, the effect of molar mass on the second virial coefficient will overcome the effects of temperature on this same temperature. This effect can be deduced when comparing PMMA 107K at 32.6 ^{o}C to PMMA 265K at 35 ^{o}C. In another case, the effect of temperature will overcome the effect of molar mass. This can be seen when comparing PMMA 53.6K at 28 ^{o}C to PMMA 142.2K at 29 ^{o}C to PMMA 178K at 30 ^{o}C, and also when comparing the set of results for PS in cyclohexane.

The radius of gyration values shown in table 1 are calculated using the random walk model, which is a hypothesis that illustrates the structure of a polymer in solution under theta conditions. Since this model is applicable at the theta sate, the size of the polymer expressed as R_G is expected to be underestimated in the case of good solvent

($A_2>0$) and overestimated in the case of a poor solvent ($A_2<0$). The calculation of $R_{G,\theta}$ is performed according to the following equation.[57]

$$R_{G,\theta} = \sqrt{\frac{nl_0^2}{6}}$$

where *n* corresponds to the degree of polymerization of the analyte (i.e., *n*-1 is the number of steps in the random walk) and l_0 to the length of a step in the random walk. The latter are tabulated values for PS, PMMA, and a number of other polymers, the value for PS being 0.530 nm and that for PMMA 0.481 nm[7]. The degree of polymerization *n* is calculated from:

$$n = \frac{M_w}{M_o}$$

where M_o is the molar mass of a repeat unit of the polymer, 104 g/mol for PS and 100 g/mol for PMMA. We note that all of the analytes were virtually monodisperse, i.e., $\ldots M_n \approx M_w \approx M_z \ldots$ and thus virtually identical results are obtained regardless of which statistical moment is used for the numerator in the previous equation.

The viscometric radius, R_η, are calculated based on the equation shown in the introduction, where the molar mass are obtained from the manufacturer and the intrinsic viscosity is calculated from the Mark-Houwink equation at the theta state as per.

$$[\eta]_\theta = K_\theta M^{0.5}$$

where literature values for K_θ at the theta state in the solvents used in our experiments.

The R_G as well as the R_η values are calculated according to assumptions related to the polymer at the theta state. Consequently, the obtained values for R_G and R_η are not accurate in the cases where the second virial coefficient is non-zero. Thus, these values are used as an aid to qualitatively compare the different radii.

Table 1. Size and second virial coefficient data for PS and PMMA.

Polymer	**Solvent**	T (°C)	A_2[a] (mol mL g^{-2})	R_T[a,b] (nm)	$R_{G,\theta}$[c] (nm)	R_H[d] (nm)	$R_{\eta,\theta}$[e] (nm)
PS 66.5K[f]	Cyclohexane	24.0	-1.12×10^{-5}	-2	5	5	6
		28.0	-6.35×10^{-6}	-1	5	---	6
		32.0	9.20×10^{-6}	2	5	---	6
PS 68K	Cyclohexane	34.0	5.08×10^{-5}	3	6	4	6
PS 189K	Cyclohexane	34.0 (θ)	0.00×10^{-5}	0	9	8	10
PS 501.5K	Cyclohexane	35.0	1.66×10^{-4}	16	---	---	---
PMMA 53.6K	Acetonitrile	28.0	-1.43×10^{-4}	-3	5	4	4
PMMA 142.2K	Acetonitrile	29.0	1.31×10^{-5}	3	7	6	6
PMMA 177.8K	Acetonitrile	29.0	-6.52×10^{-5}	-6	8	---	8
		29.2	-8.86×10^{-5}	-6	8	6	8
		30.0	2.28×10^{-5}	4	8	---	8
PMMA 107K	*n*-butyl chloride	32.6 (~θ)	9.72×10^{-6}	2	6	6	7
PMMA 265K	*n*-butyl chloride	35.0	-4.67×10^{-5}	-7	10	9	12

[a]Measured using off-line MALS.

[b]Calculated using appropriate equation in text.

[c]Theta-state value calculated using Equation 1 in text.

[d]Based on DLS measurement of D_T; R_H calculated using appropriate equation in text.

[e]Theta-state value calculated using Equation 3 in text in combination with R_η equation in Table 1.

[f]PS 66.5K denotes a narrow polydispersity linear polystyrene standard with weight-average molar mass, M_w, of 66500 g/mol. Same nomenclature is followed for the other polymers, with PMMA denoting poly(methyl methacrylate).

Conclusions

In this project, we have successfully reported experimental evidence of negative thermodynamic radii. The explanation of the negative values obtained for this hard-sphere equivalent radius is related to the second virial coefficient on which this radius depends. This second virial coefficient is a measure of the excluded volume of a polymer in solution defined as the difference between the size of a polymer occupied at certain solvent/ temperature conditions and that occupied at theta state. Besides being negative, the thermodynamic radius can be zero at the theta state, as shown experimentally. To our knowledge, we are the first to report negative and zero values for the thermodynamic radius. For the sake of comparison, three more radii are reported: 1) The radius of gyration (R_G). 2) The viscometric radius (R_η). 3) The hydrodynamic radius (R_H). These three radii possess positive values under all conditions, in contrast to the thermodynamic radius, as discussed above.

We hope that we have provided a better understanding of the term "size" of a polymer in solution by introducing the negative radius concept supported by experimental values. We also hope that this project will help in understanding the properties of polymers.

REFERENCES

1. Balsara, N. P.; Tirrell, M.; Lodge, T. P. *Macromolecules* **1991,** 24, (8), 1975-86.

2. Ding, J.; Tao, Y.; Day, M.; Roovers, J.; D'Iorio, M. *Journal of Optics A: Pure and Applied Optics* **2002,** 4, (6), S267-S272.

3. Huang, H.; He, Q.; Lin, H.; Bai, F.; Cao, Y. *Thin Solid Films* **2005,** 477, (1-2), 7-13.

4. Lee, M. S.; Lodge, T. P.; Macosko, C. W. *Journal of Polymer Science, Part B: Polymer Physics* **1997,** 35, (17), 2835-2842.

5. Burchard, W., *Advances In Polymer Science*. In **1999**, 143, 113-194.

6. Stockmayer, W. H.; Moore, L. D., Jr.; Fixman, M.; Epstein, B. N. *Journal of Polymer Science* **1955,** 16, 517-30.

7. Clarke, C. J.; Eisenberg, A.; LaScala, J.; Rafailovich, M. H.; Sokolov, J.; Li, Z.; Qu, S.; Nguyen, D.; Schwarz, S. A.; Strzhemechny, Y.; Sauer, B. B. *Macromolecules* **1997,** 30, (14), 4184-4188.

8. Angerman, H.; Hadziioannou, G.; Tenbrinke, G. *Physical Review E* **1994,** 50, (5), 3808-3813.

9. Russell, T. P.; Hjelm, R. P.; Seeger, P. A. *Macromolecules* **1990,** 23, (3), 890-893.

10. Kotaka, T.; Murakami, Y.; Ingaki, H. *Journal of Physical Chemistry* **1968,** 72, (3), 829-841.

11. Kent, M. S.; Tirrell, M.; Lodge, T. P. *Journal of Polymer Science Part B-Polymer Physics* **1994,** 32, (11), 1927-1941.

12. Kent, M. S.; Tirrell, M.; Lodge, T. P. *Macromolecules* **1992,** 25, (20), 5383-5397.

13. Aliyar, H. A.; Hamilton, P. D.; Ravi, N. *Biomacromolecules* **2005,** 6, (1), 204-211.

14. de Groot, J. H.; van Beijma, F. J.; Haitjema, H. J.; Dillingham, K. A.; Hodd, K. A.; Koopmans, S. A.; Norrby, S. *Biomacromolecules* **2001,** 2, (3), 628-634.

15. Lai, Y.-C.; Valint, P. L., Jr. *Journal of Applied Polymer Science* **1996,** 61, (12), 2051-2058.

16. Robertson, J. R.; US Patent 330616, 19890216, **1989**.

17. Hiratani, H.; Baba, M.; Yasui, T.; Ito, E.; Yung, L.-Y. L. *Journal of Applied Polymer Science* **2003,** 89, (14), 3786-3789.

18. Ketelson, H. A.; Meadows, D. L.; Stone, R. P. *Colloids and Surfaces, B: Biointerfaces* **2005,** 40, (1), 1-9.

19. Khokhlov, A. R.; Khalatur, P. G. *Physica A* **1998,** 249, (1-4), 253-261.

20. Khokhlov, A. R.; Khalatur, P. G. *Physical Review Letters* **1999,** 82, (17), 3456-3459.

21. Lozinskii, V. I.; Simenel, I. A.; Khokhlov, A. R. *Doklady Chemistry* **2006,** 410, 170-173.

22. Lozinsky, V. I.; Simenel, I. A.; Kulakova, V. K.; Kurskaya, E. A.; Babushkina, T. A.; Klimova, T. P.; Burova, T. V.; Dubovik, A. S.; Grinberg, V. Y.; Galaev, I. Y.; Mattiasson, B.; Khokhlov, A. R. *Macromolecules* **2003,** 36, (19), 7308-7323.

23. Ermoshkin, A. V.; Chen, J. Z. Y.; Lai, P. Y. *Physical Review E* **2002,** 66, (5), 6.

24. Chen, H.; Wang, C.-G.; Ying, L.; Cai, H.-S. *Journal of Applied Polymer Science* **2004,** 91, (6), 4105-4108.

25. Nassar, A. M.; Ahmed, N. S. *International Journal of Polymeric Materials* **2006,** 55, (11), 947-955.

26. Qureshi, G. J.; Padha, N.; Gupta, V. K.; Kamalasanan, M. N.; Singh, A. P.; Kapoor, A.; Tripathi, K. N. *Optics & Laser Technology* **2003,** 35, (5), 401-407.

27. Ghawana, K.; Singh, S.; Tripathi, K. N. *Journal of Optics-Nouvelle Revue D Optique* **1998,** 29, (4), 265-267.

28. Kim, H. J.; Kim, K.; Chin, I.-J. *Molecular Crystals and Liquid Crystals* **2007,** 463, 383-388.

29. Kim, D. H.; Lau, K. H. A.; Robertson, J. W. F.; Lee, O. J.; Jeong, U.; Lee, J. I.; Hawker, C. J.; Russell, T. P.; Kim, J. K.; Knoll, W. *Advanced Materials* **2005,** 17, (20), 2442-2446.

30. Black, C. T.; Ruiz, R.; Breyta, G.; Cheng, J. Y.; Colburn, M. E.; Guarini, K. W.; Kim, H. C.; Zhang, Y. *IBM Journal of Research and Development* **2007,** 51, (5), 605-633.

31. Thurn-Albrecht, T.; Steiner, R.; DeRouchey, J.; Stafford, C. M.; Huang, E.; Bal, M.; Tuominen, M.; Hawker, C. J.; Russell, T. P. *Advanced Materials* **2000,** 12, (11), 787-790.

32. Wang, J.-Y.; Leiston-Belanger, J. M.; Sievert, J. D.; Russell, T. P. *Macromolecules* **2006,** 39, (24), 8487-8491.

33. Park, D.-H. *Nanotechnology* **2007,** 18, (35), 355304/1-355304/7.

34. Aissou, K.; Kogelschatz, M.; Baron, T.; Gentile, P. *Surface Science* **2007,** 601, (13), 2611-2614.

35. Adedeji, A.; Lyu, S.; Macosko, C. W. *Macromolecules* **2001,** 34, (25), 8663-8668.

36. Utiyama, H.; Takenaka, K.; Mizumori, M.; Fukuda, M. *Macromolecules* **1974,** 7, (1), 28-34.

37. Ohnuma, H.; Kotaka, T.; Inagaki, H. *Polymer Journal (Tokyo, Japan)* **1970,** 1, (6), 716-26.

38. Fukuda, T.; Nagata, M.; Inagaki, H. *Macromolecules* **1984,** 17, (4), 548-553.

39. Galvin, M. E. *Macromolecules* **1991,** 24, (23), 6354-6356.

40. Fukuda, T.; Nagata, M.; Inagaki, H. *Macromolecules* **1986,** 19, (5), 1411-1416.

41. Kennedy, J. F.; Suett, A. D., *Handbook of Size Exclusion Chromatography edited by Chi-San Wu*. Vieweg Verlag: New York, 1995.

42. Yau, W. W.; Kirkland, J. J.; Bly, D. D., *Modern Size-Exclusion Liquid Chromatography*. Wiley: New York, **1979**.

43. Striegel, A. M. *Analytical Chemistry* **2005,** 77, (5), 104A-113A.

44. Chang, T. *Journal of Polymer Science, Part B: Polymer Physics* **2005,** 43, (13), 1591-1607.

45. Wyatt, P. J. *Analytica Chimica Acta* **1993,** 272, (1), 1-40.

46. Striegel, A.; Editor, *Multiple Detection in Size-Exclusion Chromatography.* ACS Symp. Ser. 893; American Chemical Society: Washington, DC; **2005**.

47. Pethrick, R. A.; Dawkins, J. V., *Modern Techniques for Polymer Characterization*. Wiley: New York; **1999**.

48. Kalvoda, R., *Operational Amplifiers in Chemical Instrumentation*. Horwood: New York ;**1975**.

49. Itakura, M.; Sato, K.; Lusenkova, M. A.; Matsuyama, S.; Shimada, K.; Saito, T.; Kinugasa, S. *Journal of Applied Polymer Science* **2004,** 94, (3), 1101-1106.

50. Candau, F.; Francois, J.; Benoit, H. *Polymer* **1974,** 15, (10), 626-30.

51. Medrano, R.; Laguna, M. T. R.; Saiz, E.; Tarazona, M. P. *Physical Chemistry Chemical Physics* **2003,** 5, (1), 151-157.

52. Kurata, M.; Fukatsu, M.; Sotobayashi, H.; Yamakawa, H. *Journal of Chemical Physics* **1964,** 41, (1), 139-49.

53. Kawaguchi, T.; Osa, M.; Yoshizaki, T.; Yamakawa, H. *Macromolecules* **2004,** 37, (6), 2240-2248

54. Seymour, R. B.; Carraher, C. E., Jr., *Polymer Chemistry. An Introduction*. Marcel Dekker: New York; **1981**.

55. Elias, H. G.; Editor, *An Introduction to Polymer Science*. VCH: New York ; **1997**.

56. Brandrup, J.; Immergut, E. H.; Editors, *Polymer Handbook, Fourth Edition*. Wiley: New York; **1998**.

57. Hiemenz, P. C. *Polymer chemistry - The basic concepts*, Marcel Dekker, New York, **1984**.

58. De Gennes, P. G., *Scaling Concepts in Polymer Physics*. Cornell University Press: Ithaca, N.Y.**1979**.

59. Smith, M. J.; Haidar, I. A.; Striegel, A. M. *Analyst* **2007,** 132, (5), 455-460.

60. Mourey, T. *International Journal of Polymer Analysis and Characterization* **2004,** 9, (1-3), 97-135.

61. P. J. Flory. *Principles of Polymer Chemistry*, Cornell; Ithaca, NY; **1953**.

62. Billmeyer, F. W. J. *Textbook of Polymer Science, 3rd edition*, Wiley-Interscience: New York; **1984**.

BIOGRAPHICAL SKETCH

Imad Haidar Ahmad was born in Beirut/Lebanon in 1981. He lived his childhood on his Village Ras Oasta asnd in Beirut. From 2000 till 2004, Imad went to the Lebanese University at Al-Hadath where he got his maîtrise degree in Chemistry. Imad Joined FSU in Fall 2005 as a graduate student and worked in the area of Analytical Chemistry under the supervision of Dr. André M. Striegel. Following his completion of Master's in Chemistry, Imad will continue his PhD in Analytical Chemistry.